EMBRITTLEMENT OF C46400 BRASS BY

LIQUID MERCURY

By

NARESH VENKATA LAKSHMI ADURTY

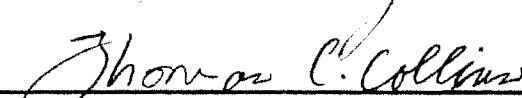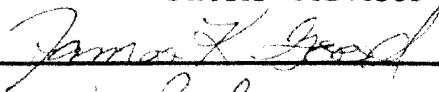Bachelor of Science

Kakatiya University

Warangal, India

1991

Submitted to the Faculty of the
Graduate College of the
Oklahoma State University
in partial fulfillment of
the requirements for
the Degree of
MASTER OF SCIENCE
MAY, 1994

EMBRITTLEMENT OF C46400 BRASS BY

LIQUID MERCURY

Thesis Approved:

_____
Thesis Advisor

_____

_____

_____
Dean of the Graduate College

ACKNOWLEDGMENTS

TABLE OF CONTENTS

LIST OF TABLES

LIST OF FIGURES

CHAPTER I

INTRODUCTION

The intent behind this study is to clarify the effects of some of the variables affecting liquid metal embrittlement (LME) in copper alloys. The experimental program is confined to C11000, C36000 and C46400 brass embrittled by liquid mercury at, and near, room temperature, but reference is made to the embrittlement of the nickel-copper alloy, alloy N04400. The variables studied specifically were wettability, heat treatment, strain rate, prior cold work and temperature. Of concern was the degree of embrittlement, whether the cracking was intergranular (IG) or transgranular (TG) and whether the cracking was time dependent. Comparisons are made to the embrittlement of aluminum and nickel alloys by liquid mercury and to the stress corrosion cracking (SCC) of brass by ammonia. The LME by mercury of nickel alloys, but not aluminum alloys, is strain rate sensitive (1, 2, 3, 4, 5). Accordingly, an indentation test for embrittlement worked with aluminum but not with nickel alloys. In the case of SCC of brass by ammonia, the cracking can be IG or TG depending on the pH (7).

Environmental embrittlement includes SCC, LME and hydrogen embrittlement. Copper alloys are not normally embrittled by hydrogen because hydrogen is not adsorbed by copper (8). An exception occurs when moisture is trapped, which reacts to give copper oxide and hydrogen that generates an internal gas pressure. SCC is an important and common

1

phenomenon, for example the cracking of austenitic stainless steels by chlorides. LME is less common but can be tragic. A recent example is the disclosure of a Russian nuclear submarine mishap where the necessity to repair a cracked cooling pipe resulted in the quick and painful death of 22 volunteers involved. The pipe cracked because of LME by molten solder, spatter that occured earlier at the dockyard (9). There are tales, probably apocryphal, of the failure of brass connections in hospitals after mercury thermometers broke. A brief review of LME follows with particular reference to copper alloys. For completeness, SCC of copper alloys by ammonia is discussed briefly.

CHAPTER II

LITERATURE REVIEW

1. LIQUID METAL EMBRITTLEMENT

Liquid Metal Embrittlement (LME) is the sudden onset of brittle failure of a solid metal in the presence of a liquid metal, where some form of ductile failure would otherwise occur. Embrittlement manifests itself as a reduction in fracture strain. The embrittlement may be severe, and the crack propagation of the fracture is often fast in the case of LME as compared to SCC. The speed of an LME crack is 10-100 cm/s in some cases (10).

According to Kamdar (10), the main characteristics that distinguish LME from other environmentally assisted cracking processes are the predominant occurrence of brittle fractures surfaces and a significant loss in ductility and strength, due to the presence of liquid at the crack tip. The fracture of a material, as the result of LME, changes from a ductile mode to a brittle IG or brittle TG mode. Fracture can occur well below the yield stress of the solid. In LME, the stress required to initiate a crack is often higher than the stress required to propagate the crack. Hence, crack initiation can lead to immediate failure.
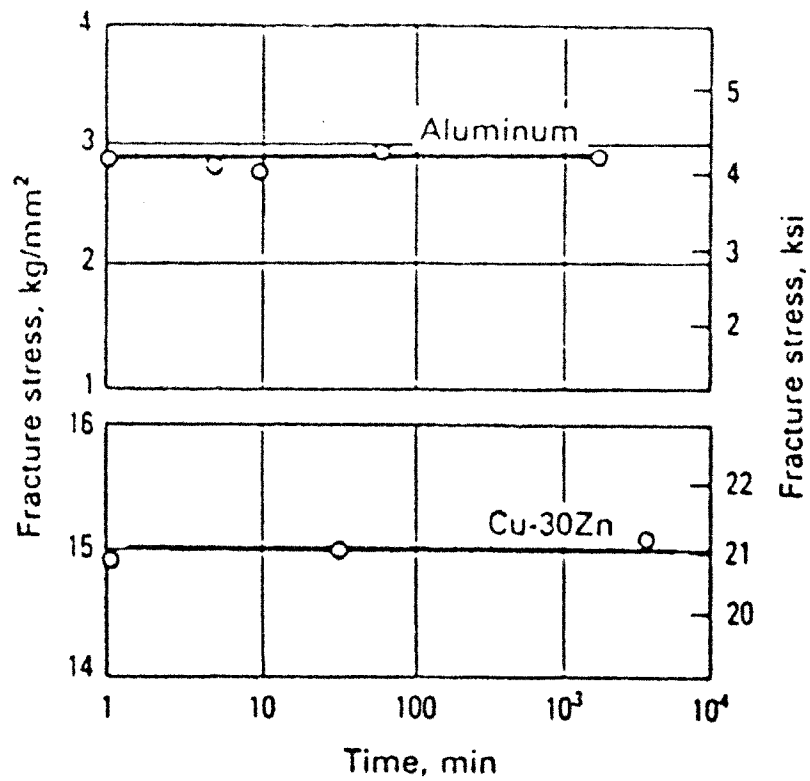
Figure 1. The plot illustrates that the fracture stress of polycrystalline aluminum and Cu-30 Zn brass is independent of the time of exposure to liquid mercury before testing in this environment (10).

1.2 ROLE OF LIQUID IN CRACK PROPAGATION

The crack propagation activation energy for brass in liquid mercury is only 3 to 5 kcal/mol (13). This corresponds to the diffusion of liquid mercury over mercury adsorbed on brass. The very high velocities of crack propagation and very low activation energies are considered to be distinguishing features from SCC in the same metal.

1.3 MECHANISMS OF LME

There are many models proposed on the micro mechanism of the embrittlement at the crack tip. One of the mechanisms proposed was reduced cohesion by Stoloff (19, 20, 21). This model states that adsorption of a liquid metal atom at the crack tip effectively reduces the cohesive strength of the crack tip bond, resulting in crack growth at lower stresses. The adsorbed atoms react with the bonded atoms which form the crack tip. Assuming that the cohesive strength of these bonds determines the stress at which the crack grows, Stoloff states that the presence of the adsorbed atoms reduces the strength of the crack tip bond.

Robertson (22) proposed a mechanism which deals with very rapid dissolution of the solid metal at the crack tip. The dissolved metal must be quickly carried away from the crack tip for the reaction to proceed. But this mechanism has not been accepted at large because of the difference in the predicted and the actual effects of temperature.

A grain boundary penetration model was proposed by Kristal (23) which assumes that embrittlement occurs in two steps. Diffusion of liquid along grain boundaries causes a reduction in the grain boundary surface

energy, or strain concentrations cause dislocation emission and crack initiation. The model proposes that liquid metal atoms, adsorbed at the solid metal surface, diffuse along the grain boundaries, facilitated by applied stress. Once a sufficient concentration of embrittling atoms is present along the grain boundaries, the surface energy of the grain boundary is reduced sufficiently to cause embrittlment. This model fails to explain the TG fracture which has often been observed.

Lynch (24, 25) proposed an enhanced plastic deformation model for LME. After studying the metallography and fractography of LME in zinc single crystals, nickel single crystals and a quenched and tempered steel (D6ac) in a liquid mercury environment, he claimed that liquid metal atoms adsorbed at the crack tip do not facilitate decohesion; rather, they enhance dislocation emission from the crack tip. The enhanced plasticity model states that adsorbed liquid metal atoms at the tip locally change the properties at the crack tip bond. The potential energy is decreased and so is the shear modulus. The nucleation of the dislocation is facilitated by the reduced shear strength at low stresses.

1.4 FACTORS EFFECTING LME OF COPPER AND COPPER ALLOYS BY MERCURY

LME can be regarded as a special case of brittle fracture because it causes a reduction in the fracture stress (26, 27). Therefore, the factors which tend to enhance brittle fracture in an inert environment would similarly increase the susceptibility and severity of brittle fracture in the active liquid metal environment. These factors include coarser grain size, prior cold work, and

8

decreased temperature. In the case of copper-zinc alloys, the percentage of zinc also effects the embrittlement.

1.4.1 EFFECT OF Zn CONTENT ON LME OF Cu-Zn ALLOYS

Edmunds, Anderson and Waring (28) prepared specimens, ranging from 57%-97% Cu, in order to study the effect of the Cu-Zn ratio on embrittlement by liquid mercury. All specimens were 1/4 x 2 x 4 in. closed-mold slabs which were sanded smooth, then cold-rolled directly to a thickness of 0.035 in. The strength of the alloy increased up to 20% Zn and afterwards there was no significant change with the addition of Zn up to 40%. They found that as rolled specimens containing 75%-100% Cu showed an increase in mercury-cracking resistance with increase in Zn content. The alloys higher in Zn content, i.e. above 25% were significantly affected by mercury. Figure 2 shows the effect of Zn on fracture stress during LME of copper alloys.

Edmund (29) found that the susceptibility to failure increased with zinc content in the range of 10 to 40 % Zn. Whitaker (30) performed tests on extruded α, α plus β, and β brasses containing aluminum and coated with molten eutectic Pb/Sn solder at 200°C. He observed that during embrittlement of β alloys, inter crystalline attack was most severe. In the α plus β alloys, the inter crystalline attack was less severe and the penetration generally follows a path through the α areas.

At one time there was conflicting opinion on the embrittlement of pure Cu by mercury. Robertson (31) did tests on oxygen free copper and brass (69% Cu) at 170°C and reported that pure copper was not embrittled by mercury, whereas brass was. Moore et al (15) observed that copper was not embrittled by Hg.
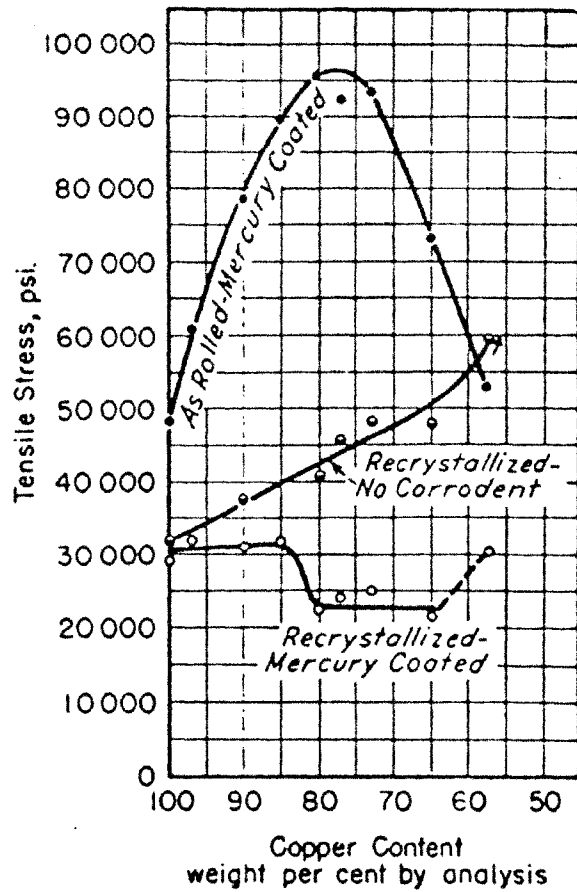
Figure 2. The copper content of brass versus its tensile breaking stress when coated with mercury (29). Note that the embrittlement increases significantly as the zinc content increases beyond 15%.

Shunk and Worke (32) listed pure copper as a metal that was embrittled by mercury. Davies et al (33) reported a 25% loss in uniform elongation when tested in Hg as compared to tests in air. Tiner (34) and, Rosenberg and Cadoff (35) also observed that copper suffered embrittlement by Hg in both tensile and fatigue tests respectively. Peevy (36) also observed the embrittlement of C1100 copper under tensile testing. Greenwood (37) observed that copper was embrittled by mercury and the fracture were IG. Since the breaking stress was only slightly reduced, it was suggested by Greenwood (37) that this might have been the reason why embrittlement was not observed by other workers.

1.4.2 EFFECT OF GRAIN SIZE

Copper and copper alloys, when tested in air do not exhibit much grain size dependence on fracture. However, when tested in appropriate liquid metal environments, like mercury on brass, these metals can fail in a brittle manner and obey the Cottrell-Petch equation (38, 39):

$$S_y K_y d^{1/2} = bmg \dots\dots\dots\dots\dots\dots\dots\dots\dots\dots\dots(1)$$

which is a relationship defining the ductile-brittle transition of a solid. Here, S_y is the yield strength of the solid, d is the grain size, m is the shear modulus, g is the effective fracture energy, and K_y and b are geometric factors, relating to dislocation generation and the stress state effects, respectively. If the left side of the equation becomes greater, brittle fracture is expected. It is observed from this equation that an increase in the grain size favors brittle failure, thus the embrittlement. This is shown in Figure 3.

Grain boundaries constitute an obstacle to plastic flow and therefore are potential sites for stress concentration. The magnitude of the stress concentration is related to the pile-up lengths. A smaller grain size means a lower stress concentration at the dislocation pile-ups at the grain boundaries, and therefore a greater amount of embrittler penetration is required to accomplish the necessary lowering of crack resistance (40).

Davies et al (33) suggest that discrepancies as to the degree of embrittlement of pure copper by mercury, at least in part, are due to the influence of grain size on embrittlement. Kamdar (27) observed that pure copper was embrittled by mercury only when the metal possessed a coarse grain size.

1.4.3 EFFECT OF PRIOR COLD WORK

For a pure copper, the fracture stress usually increases approximately linearly with prestrain. But for the fine grained material or strain aging alloys, such as 70:30 brass, the effects of prestrain are not always those anticipated.

The effect of prior cold work on LME is not understood completely. Rinnovetore et al (41) found that a tensile prestrain increases the susceptibility to embrittlement of α brass in the presence of liquid mercury. Where as Pidathala (42) found that in case of free cutting brass, for initial amounts of compressive prestrain i.e. up to 25% true strain cold work, the severity of the embrittlement increased with the increase in the cold work, but after 25% prestrain the severity of embrittlement decreased with the increase in the cold work. The mode of cracking was found to be TG.

Similar behavior was observed by Rinnavatore et al (36), with maximum embrittlement occurring at 22% true strain. The tests were done on cold rolled α brass in the presence of Hg-Na amalgam. But here, the mode of cracking was IG for the cold work less than 22% and TG for the cold work greater than 22%. For larger amounts of cold work, around 90% reduction in area, practically no embrittlement was observed. Elimination of the grain boundaries resulting from the cold work is stated to be the dominant factor responsible for the change in the susceptibility to embrittlement and fracture mode.

1.4.4 EFFECT OF TEMPERATURE

The maximum LME usually occurs at or a little above the melting point of the embrittler and, DBTT (ductile-to-brittle transition temperature) occurs as the temperature increases (44). The temperature at which ductility starts decreasing and the temperature at which ductility starts increasing again are sometime defined as T_E and T_R respectively. Thus, a ductility trough over a particular temperature range can be seen in Figure 4. Nicholas and Rostoker (45) found that the width and the depth of the trough varies from system to system and some times on the strain rate used during the tests on a given system. The width of the trough also depends on the grain size. It was observed that the width of the trough increased with an increase in grain size in the 70-30 brass (45). All recovery temperatures in this alloy were well above the room temperature. For the grain size varying from 0.003 mm to 0.055 mm, they found the trough width ranging from 75 °C to 160 °C (Figure 5).

13

Mercury Stress-Cracking Tensile Breaking Stress, psi.

28 000

26 000

24 000

22 000

20 000

18 000

Mercury Stress-Cracking

8

Ammonia Stress-Cracking Time to Failure, min. at 10 000 - psi. Stress

500

400

300

200

100

Ammonia Stress-Cracking

0   0.02   0.04   0.06   0.08   0.10   0.12

Average Grain Diameter, mm.
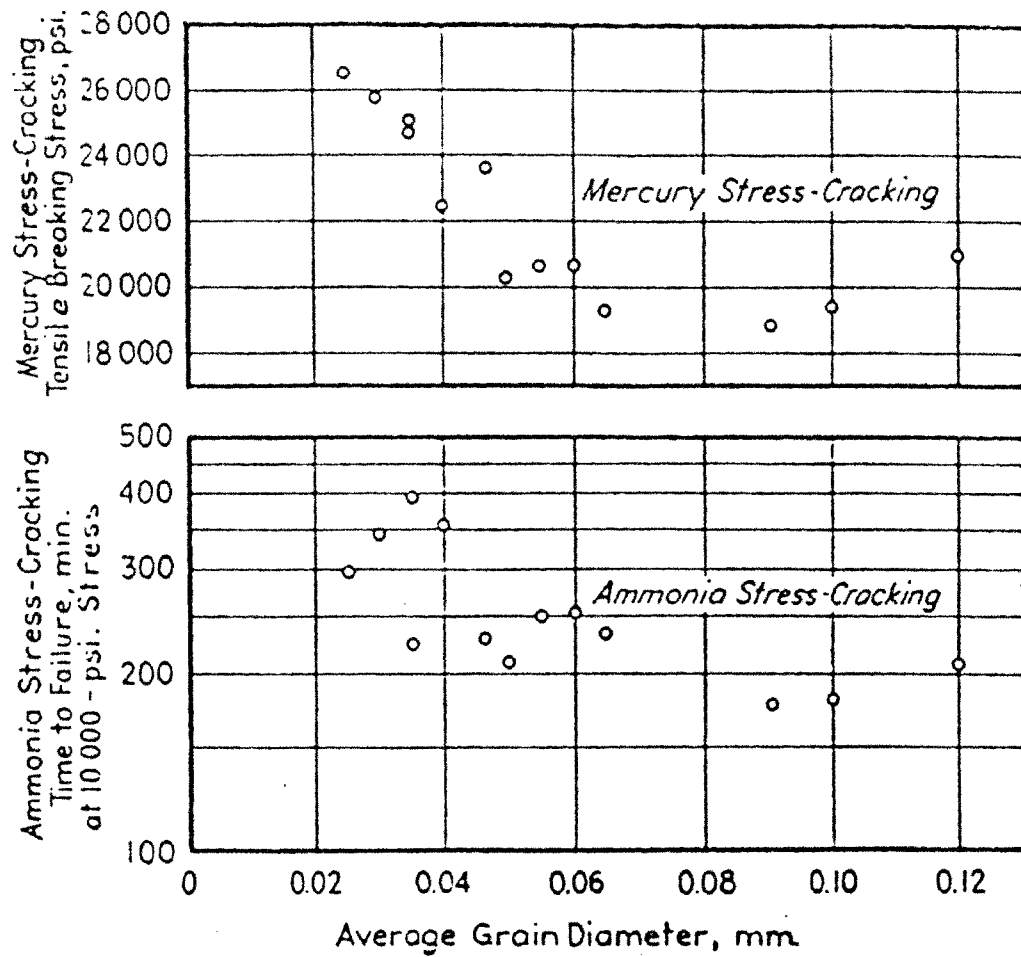
Figure 3. The variation of mercury embrittlement and SCC of recrystallized C26000 with the grain size (29). Note the embrittlement increases with the increase in grain size.

Kamdar (16) stated that the temperature affects the susceptibility of liquid metal embrittlement in two ways,

1) The crack tip becomes blunted at elevated temperatures, either because of the increased ductility resulting in the decreased yield stress of the metal, or due to dissolution at the tip into the liquid metal environment.

2) The rate of arrival or diffusion of liquid metal atoms to the propagating tip could be affected by temperature. A higher temperature goes with lower surface tension, which means a higher degree of wettability and smaller "critical radius" of penetration.

Hence, it can be concluded that at higher temperatures it is more difficult to initiate or propagate a brittle crack in a solid whose yield stress would be reduced with increase in temperature. At lower temperatures, the surface tension of the liquid metal will be higher and the wettability will be lower, hence, the transportation of liquid metal atoms to the crack tip becomes difficult thus reducing the severity of LME. Therefore the maximum embrittlement will occur at intermediate temperatures where the embrittler liquid atoms can be transported to the crack tip without the blunting of the crack tip.

2. STRESS CORROSION CRACKING

SCC is a spontaneous cracking which results from the combined effect of stress, and corrosion. SCC was observed in India in the last century, in the form of season cracking of cartridge brass. The most extensive systematic study of SCC of brass is by Mattsson (7).
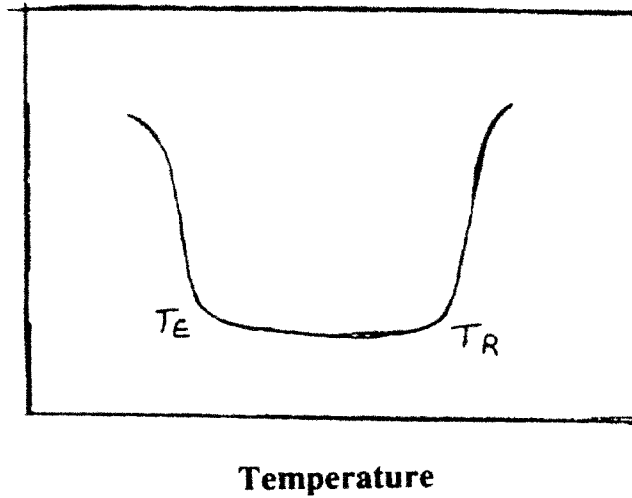
Temperature

Figure 4. Effect of LME on the variation of ductility with temperature (44). T_E is the temperatures at which ductility starts decreasing and T_R is the recovery temperature.
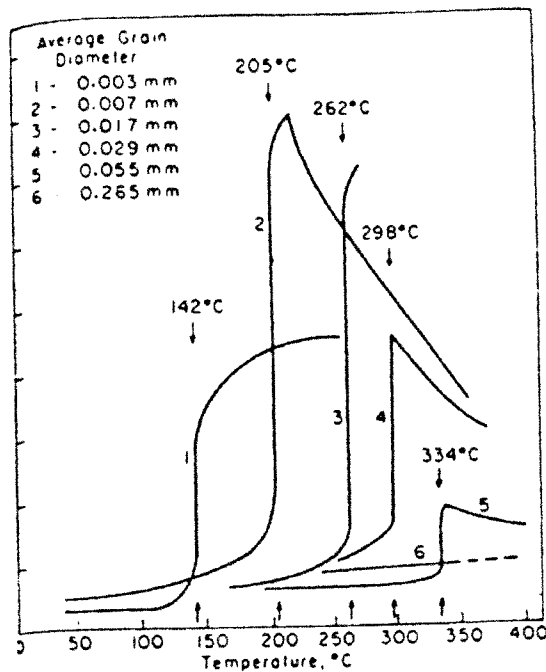
Figure 5. Curves of transition from brittle to ductile behavior of 70/30 brass wetted with mercury at various grain sizes (45). Recovery temperature of the alloy is dependent on the grain size and is well above the room temperature.

16

The consequences of this can be serious in the application of brass generally, for example, with cartridge cases. Cartridge cases often contain residual stresses. Their failure from this cause may allow the escape of gas from the gun breech, a hazard to the shooter, and may not eject, thus temporarily putting the gun out of action. In loaded cartridge cases, the stress present is partly residual and partly applied by the insertion of the projectile. Ammonia, present as a decomposition product of smokeless powder, air, and moisture constitutes the corrosive media (28).

It was also observed that brasses stored in a dry, and clean atmosphere, although carrying high internal stresses, cracked only after a long time, while a damp atmosphere was especially active in producing such cracking, particularly if it carried ammonia vapor from decaying organic matter (28).

2.1 EFFECT OF GRAIN SIZE

Edmunds (29) found that there was a correlation between the grain size and the time to failure by stress corrosion cracking (Figure 3). There is an increase in time-to-failure with the decrease in grain size in the range of 0.08 mm to 0.02 mm. The attack by ammonia, though preferentially IG can also be TG.

For a further examination of the influence of grain size, Edmunds (22) used specimens of extra hard rolled commercial cartridge brass (C26000), which were annealed for 30 minutes at temperature intervals of 50°C, from 200 to 800°C, and quenched. He tested it for ammonia stress cracking resistance (Figure 6) and found that a marked reduction in stress cracking resistance occurred coincidentally with re-crystallization. A higher annealing

17
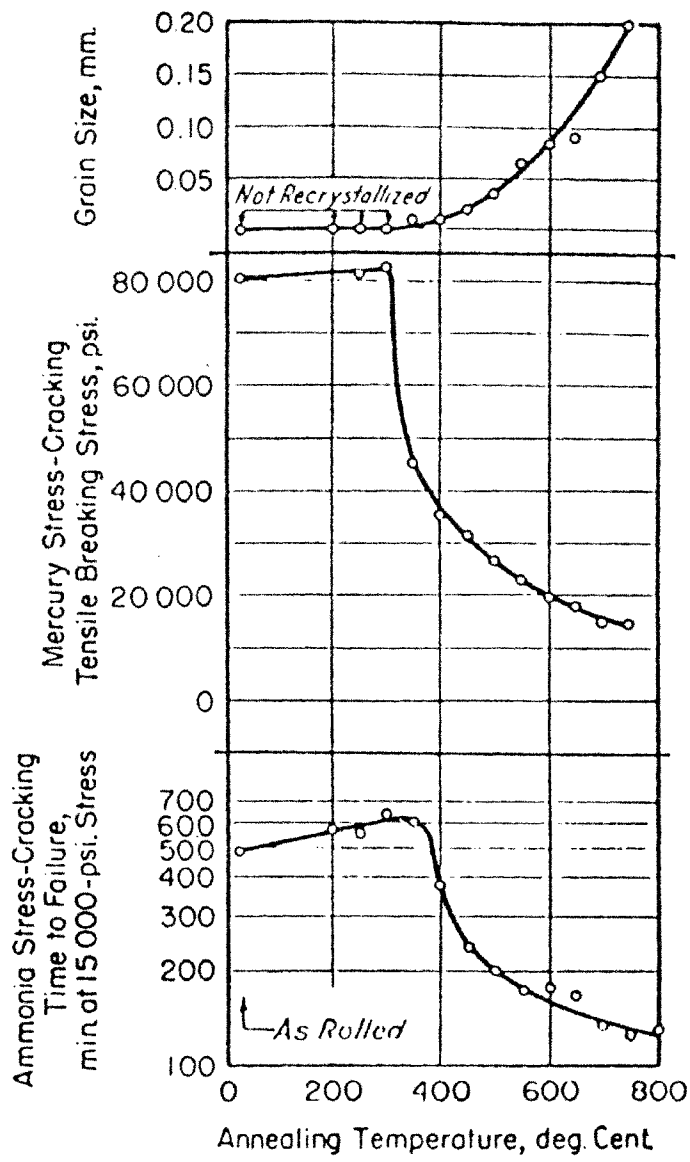
Figure 6. Effect of annealing on ammonia stress cracking and mercury stress cracking of 28000 (29). The data shows that a marked reduction in stress-cracking resistance occurs coincidentally with recrystallization.

18

temperature and the corresponding larger grain size resulted in a further loss to SCC.

Morris (46), using 3/8 inch diameter specimens, found an increase of ammonia stress cracking susceptibility with increasing grain size on C28000 and C46400.

2.2 EFFECT OF ZINC CONTENT

The strength of Cu-Zn alloys increases with the zinc content up to 20 % zinc but there is no further significant increase in strength with additional zinc up to 40 % (29).

Ammonia SCC failure in the recrystallized α brass were found to be almost wholly IG. In the α-β brass, the fracture was mainly TG passing through both α and β grains (Figure 7) (29).

Suzuki and Hisamatsu (47) studied the SCC of 99.999 % pure copper and Cu-Zn alloys containing up to 10 wt % Zn in an ammonium hydroxide solution, and found that the path of cracking was TG for pure copper and alloys containing less than 1.3 wt % Zn but IG for alloys containing greater than 1.3 wt % Zn.

Figure 8 shows that there is a decrease in ammonia stress cracking resistance with the increase in zinc content. From the tests conducted at higher stresses, Edmund (29) found that brasses containing less than 20 % zinc have a high resistance to ammonia SCC.

Earlier, pure copper was thought to be resistant to SCC and was claimed so by Bassett (48), Moore, Beckinsale and Mallinson (49). But it was shown to

be otherwise by Hartley (50), Gender (51) and Cook (52). Pugh et al (53) reported on the SCC of pure copper in non-tarnishing ammonical solution using a constant load technique. The failure was partially IG and partially TG. But pure copper didn't undergo SCC in tarnishing solution (54, 55). The report of SCC of pure copper in non-tarnishing solution was later disputed by Uhlig and Denquette (56). Later Escalante and Kruger (57) reported the IG SCC of pure copper at constant load, in copper acetate. The solution was found to be tarnishing. Suzuki and Hisamatsu (47) observed the TG SCC of pure copper under constant load stress in dilute ammonical solutions.

2.3 EFFECT OF pH

Mattsson (7) identified two kinds of solutions, tarnishing and non tarnishing, according to the appearance of the sample after the test. In a tarnishing solution, 6.3< pH < 7.3, a black surface coating of cuprous oxide was observed. The time-to-cracking, was found to decrease with increasing pH, passing through minimum at pH=7.3; however, no cracking was observed at pH=2. The cracking mode was IG in tarnishing solutions and TG in non- tarnishing solutions [3.9<pH<5.5 and 7.5< pH<11.2].

Takano and Shimodaira (58) observed SCC of α brass in Mattsson's solution at pH = 7.4, but not at pH = 2 or 10. They suggested that the cracking observed by Mattsson at pH =10 was due to a mechanical failure, caused by the thinning of the sectional area of the specimen by severe corrosion.

3. SUMMARY

The conclusions from the foregoing are that copper alloys are prone to both LME and SCC in many environments. The mode of fracture in both

Figure 7. Ammonia stress-cracking failure in α–β brass (29). The cracking is TG through α and β.
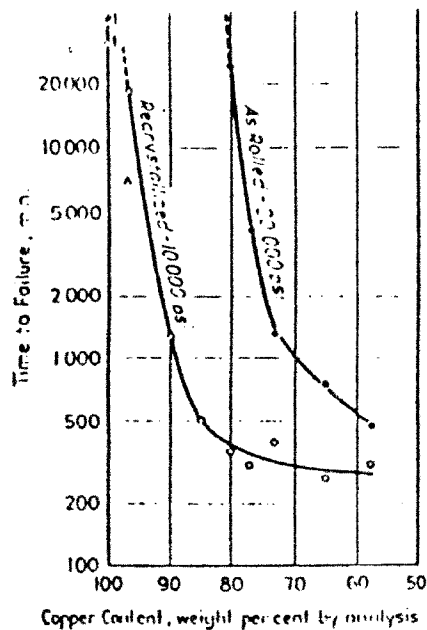
Figure 8. The copper content of brass versus its resistance to stress corrosion cracking in ammonia (29). Embrittlement increases with the increase in zinc content.

cases can be IG or TG. It is observed that Cu-Zn alloys are embrittled more than copper and that TG cracking could be through either the α or the β phase. The susceptibility to both SCC and LME increases with an increase in grain size and in zinc content.

The susceptibility to LME initially increases with the increase in the cold work, but after certain amount of prior cold work the susceptibility starts decreasing. This peak may be different for different copper alloys.

The susceptibility to SCC is effected by the pH of the solution. Maximum embrittlement occurs at pH=7.3. The cracking mode is IG in tarnishing solutions and TG in non-tarnishing solutions.

CHAPTER III

EXPERIMENTAL PROCEDURE

1. MATERIALS

The materials investigated are naval brass (C46400), free cutting brass (C36000), and electrolytic tough pitch copper (C11000). The composition and the mechanical properties are given in Table I.

The material was supplied in the form of cold drawn round bar stock, 12.7 mm diameter. Continuous vacuum, triple distilled mercury with allowable residue of 1 part in 10 million, was used.

2. HEAT TREATMENT

Naval brass and free cutting brass were tested in both air cooled and water quenched states. The copper was annealed before testing.

The brass specimens were heated to 800°C, held there for one hour and then either cooled in air or water quenched.

The copper specimens were first placed in a cold tube furnace under mild vacuum of about 20 Pa. The furnace was then brought up to 700°C and held constant for one hour. Afterwards, the furnace was turned off with specimens remaining inside and allowed to cool to near room temperature.

3. COLD WORK

Cold work was done in compression using an hydraulic tension testing machine (HTTM). It was done on naval brass and free cutting brass for both air cooled and water quenched conditions. Specimens of initial diameter 12.7 mm and initial height of approximately 12.7 mm were used. Cold working was done by compressing the specimens to different degrees. True strain was used as a measure of the cold work. It was calculated by using the following equation

$$\varepsilon_T = 2 \ln (D_0 / D) \dots\dots\dots\dots\dots\dots\dots\dots\dots\dots (2)$$

where ε_T is true strain,

      D_0 is initial diameter and

      D is final diameter after cold work.

4. SPECIMEN PREPARATION

The specimens were ground through 600 grit paper and polished using 5μm alumina. Then, the specimens were etched. The etchant comprised 10 gm $FeCl_3$, 40 ml HCl, and 100 ml water (60). Copper specimens were chemically polished for a period of five minutes in a solution of 20 volume % nitric acid, 55 volume % phosphoric acid and 25 volume % glacial acetic acid (60).

5. WETTING

24

Wetting tests were done on air cooled specimens of the three alloys. Specimens of 12.7 mm diameter and approximately 12.7 mm high were used. These tests were done at room and lower temperatures. The tests at room temperature were done on both etched and unetched samples. All tests at lower temperatures were done on etched specimens.

Different temperatures to approximately $-14^\circ C$ were obtained in the freezer using a thermostat and the tests at those temperatures were done within the freezer. To get temperatures below $-14^\circ C$, dry ice was used and the tests were performed inside the insulation box containing dry ice. Before doing the wetting tests, the specimens as well as the mercury, were maintained at the same temperature. Care was taken while handling mercury in order to avoid any spillage. The wetting tests were carried out in a petri dish placed in a plastic bag to contain any mercury that might roll off the specimens.

Wetting was tested by placing a drop of mercury on the surface of the sample, and observing its spreading. To measure temperatures accurately, a digital thermometer was used. It was calibrated at the freezing points of water and mercury. The thermometer was calibrated against other thermometers at room temperature.

There is an exponential increase in vapor pressure of mercury with an increase in temperature. Data are given in Table II (61). Because vapor pressure is significant above room temperature, tests were avoided.

6. INDENTATION TESTS

Table I. Composition and typical mechanical properties of C11000, C36000 and C46400 (59).

Material	Composition %	Tensile strength [*] MPa (ksi)	Yield strength[*] MPa (ksi)	Elongation in 50 mm (2 in.)[*], %
C11000	99.95 Cu 0.04 O	220-380 (32-55)	69-342 (10-44)	10-55
C36000	61.5 Cu 35.5 Zn 3 Pb	340-470 (49-68)	125-360 (18-52)	18-53
C46400	60 Cu 39.2 Zn 0.8 Sn	393-517 (57-75)	172-393 (25-57)	20-47

[*]*The range encompasses the properties in annealed, as well as in cold worked conditions.*

Indentation tests were done with the HTTM using a 10 mm diameter steel ball. The HTTM was calibrated by performing tensile tests on different alloys (Appendix I) and comparing the results with like tests on a different tensile machine, an MTS model 410.31, that had been calibrated using a load cell. An appropriate load cell was not available to calibrate the HTTM directly. The tensile strengths obtained on the HTTM were within 5% of the MTS values, erring on the higher side. The accuracy for repeatability was $\pm$ 0.9 kN (200 lbs). Specimens of 12.7 mm diameter and approximately 12.7 high were used. The test specimens, which had a thin film of mercury on the surface as a result of wetting, were placed in a plastic bag to collect mercury drops, in case they rolled off the surface.

The wetted specimens were placed under the indentor and the load was applied slowly. The surface was observed carefully for any crack initiation, and the corresponding load was noted. The run time for these test was 10 to 12 seconds.

The parameters varied for the indentation tests were cold work, heat treatment and temperature. Specimens maintained at lower temperatures were transferred to the testing bench in an insulation cup within 5 seconds.

7. SLOW STRAIN RATE TESTS

The tensile tests were performed on a 410.31 model MTS machine with wedge grips using air cooled waisted specimens of the geometry shown in Figure 9. The diameter of the thinnest section was 6.25 mm. The reason for

Table II. Vapor pressure of liquid mercury (61).

°C	10^3p, mm Hg	°C	10^3p, mm Hg	°C	10^2p, mm Hg
0.0	0.1846	39.7	5.034	68.9	5.20
7.1	0.3677	46.2	5.966	74.5	7.51
19.6	1.138	50.8	13.31	74.6	7.59
19.9	1.165	59.8	26.8	86.2	16.7
30.2	2.806			99.3	36.5
35.5	4.285			154.4	490

reducing the diameter along the gage length was to localize the fracture zone while avoiding any significant stress concentration. Also, any cracks found subsequently that were not at the waist would signify that crack initiation did not lead immediately to failure. The specimens were machined on a central lathe which has hydraulic copying attachment. A template was used to produce the required dimensions of the specimen. The total length of the specimen was approximately 130 mm (sufficient enough to grip in the jaws) with the length of the waisted section being approximately 35 mm.

The tests were done under displacement controlled, with a machine setting of 20% stroke, 50% load and 100% strain. The clean specimen was loaded on the MTS carefully, ensuring that it was held tight without slipping in the jaws. The tests in air were done at strain rates of 9×10^{-3} and 9×10^{-4} with an initial preload of 1kN. The center of the specimen was marked for reference to note the change in diameter at regular intervals; the corresponding peak loads were noted. These data are useful for verifying the stress-strain curve. Tensile stress is given by

$$\sigma_{ult} = P/A \dotfill (3)$$

where σ_{ult} = tensile stress,

    P=peak load and

    A= initial area of cross section.

The tests were done in a mercury environment to check whether the alloy was strain rate sensitive to LME. Before gripping the specimens in the jaws, they were etched and then passed through the holes provided in a
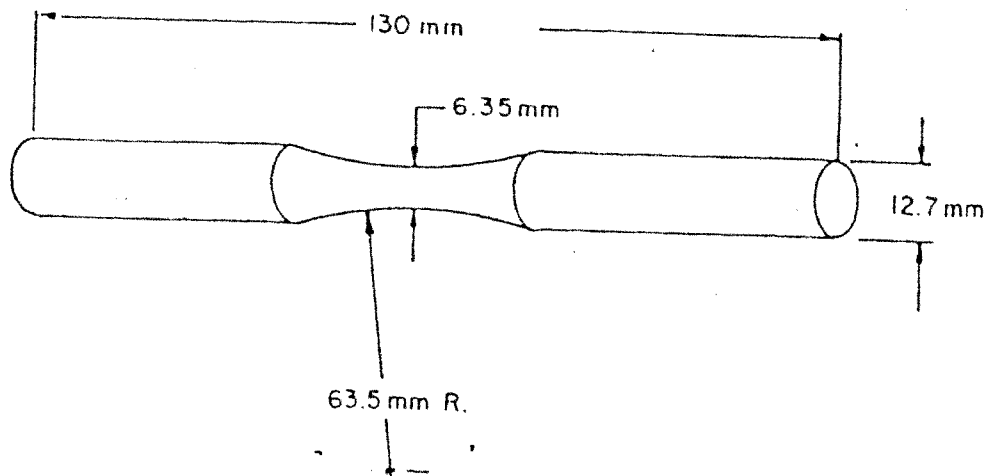
Figure 9. Geometry of the waisted tensile specimen with experimental dimensions. Waisted specimen was used in order to localize the fracture zone while avoiding any significant stress concentration.

plexiglas container as shown in the Figure 10, and then gripped in the bottom jaw. Then mercury was poured in the container to well above the waist of the specimen. The container was covered with a lid and a plastic bag was tied around the container with a rubber band to contain the mercury if any spillage occurred. Then, the specimen was held in the upper jaw. After the tests, care was taken while removing the broken specimen, in order to avoid any spillage of mercury. The tests were done at different strain rates in the mercury environment.

8. STRESS CORROSION CRACKING

For comparison purposes, indentation tests were done on naval brass in an ammonia environment. Specimens of 12.7 mm diameter and approximately 12.7 mm high were used. Four sets of tests were done. In the first set of tests, the specimens were immersed in an 80 percent NH_4OH solution for three hours, in the second for 76 hours and in the third for 168 hours, before indentation tests were done on them. In the fourth set of experiments, specimens were first indented under the compressive load of 9,000 lb. and then immersed in the 80 percent NH_4OH solution for 168 hours. These were done with the recognition that there is time factor for SCC (28).

9. METALLOGRAPHY

In order to study the specimens, it was necessary to remove the adhering mercury. Different techniques were tried to remove the mercury.
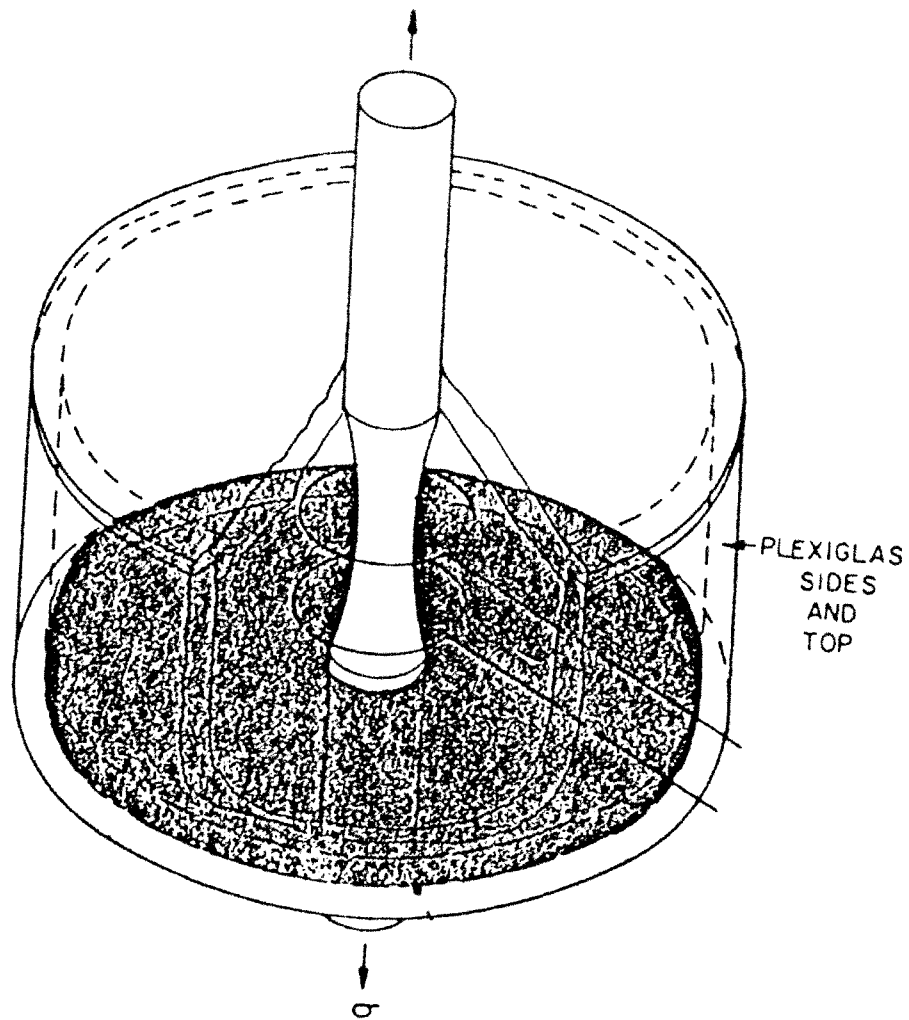
Figure 10. Plexiglas chamber to hold mercury during the tensile test. During the test, a plastic bag was tied around the container with a rubber band to contain the mercury if any spillage occured. The tests were done at different strain rates in the mercury environment.

Firstly, the mercury coated fracture surface was dipped in sulfur powder for 12 hours, such that it formed a sulfide which could be removed by swabbing with cotton. A second attempt was made to remove the mercury by heating and cooling in a closed system. Both methods were not successful because of the reason that there was a deposition of a black layer on the fractured surfaces in both cases, which may be due to formation of mercury compounds. ASTM specification B154 (02.01), which deals with the standard test methods for mercurous nitrate test for copper and its alloys, was also reffered to. Even that did not give directions to get rid of the adherent mercury layer from the samples. So, optical microscopy was done as described below.

The fractured specimens from the tensile test were vertically cut along the midsection to a depth of about 12 mm from the fractured surface, and cold mounted. Specimens from the indentation tests were cold mounted without sectioning. Then the mounted specimens were polished on emery papers of various grit sizes ranging from 240-600 and then buffed using 5 μm alumina, 0.3 μm alumina and finally 0.05 μm alumina. In order to prevent the drainage of mercury, emery papers were wetted with water before polishing the samples, rather than using continuously flowing water. Used emery papers were stored in a safe place. The specimens were etched for about a minute, washed thoroughly with flowing water and finally cleaned with methanol before drying.

CHAPTER IV

RESULTS

1. WETTING TESTS

When a drop of mercury was placed on the surface of the unetched specimens, the drop remained for approximately three minutes on the unetched surface before it began to spread on the surface. Once the mercury wet the surface, it formed an adherent layer. The mercury spread immediately on the etched surface of the samples, at room temperature. Figure 11 and Figure 12 illustrate the difference in the wetting phenomenon of the alloy with and without prior etching. Figure 11 shows the spreading of mercury after two seconds when a drop of mercury was placed on an etched surface and the whole surface was wetted in 6-10 seconds. Figure 12 shows the drop of mercury placed on an unetched surface which remained as the drop for at least three minutes before it started spreading.

When drops of mercury were placed on the samples maintained at lower temperatures, some of the drops rolled off from the surface. For the remaining drops it took approximately 2 to 6 minutes to spread thoroughly on the surface depending on the temperature, the lower the temperature, the longer the time to spread. The exact time for spreading at each temperature was difficult to record since the tests were done inside the freezer. Figure 13

shows the spreading of mercury drop on the surface of the sample maintained at 1°C, after one minute.

Similar results were obtained for C36000, but in the case of C11000 copper, slower wetting was observed in all conditions. Moreover, the mercury layer adhering to the copper surface, came off by ultrasonic cleaning whereas in case of brass, the adhering mercury layer remained to surface. Moreover, no cracks were found in any of the C11000 specimens after the indentation tests.

2. INDENTATION TESTS FOR THE EFFECT OF HEAT TREATMENT

It was observed that water quenched samples were more susceptible to embrittlement than the air cooled samples in C46400 as well as C36000. The results from both these tests are shown in Figure 14.

The crack originated at the edge of the specimen and propagated through the height of the specimen which meant that the fracture propagated simply by the progressive rupture of atomic bonds and creation of new surface. In case of the specimen, which was totally ruptured, the fracture surface was covered with mercury. Some specimens had multiple cracks on the surface. Microscopic observation revealed that water quenched samples had more β than the air cooled specimens. Mode of cracking was TG, passing through the β phase.

3. TENSILE TESTS IN AIR AND MERCURY

The stress strain curve obtained from the slow strain test of C46400 in air at a strain rate of 9×10^{-3} is shown in Figure 15. The tensile strengths obtained from the slow strain rate tests at different strain rates, in air and in mercury are shown in Figure 16. As anticipated, no strain rate sensitivity was observed in air. It was also found that the specimens tested in mercury environment failed at similar loads, thus demonstrating minimal strain rate sensitivity in mercury. The stress to failure was well below that of the stress in air (less than 50% then that of air) which meant that there was a drastic reduction in the strength of the alloy. The failure occured below the yield strength of the alloy.

The mode of cracking was TG with the cracks following the β phase (Figure 17). No side cracks were observed, away from the fracture surface, which meant that crack initiation led to failure.

4. INDENTATION TESTS FOR THE EFFECT OF PRESTRAIN

The results obtained from indentation tests done on air cooled samples, to study the effect of prestrain are shown in Figure 18. It is observed that for the initial amount of prestrain, the load to failure decreased as the degree of cold work increased, up to approximately 26% true prestrain. Then the failure load increased with the further increase in prestrain.

Similar results were obtained when the tests were done on water quenched samples. The results are shown in Figure 19. Here, the minimum in the curve is at approximately 18% true prestrain.

The mode of cracking was always TG in both air cooled and water quenched samples through the matrix, the β phase. Figure 20 shows the mode of cracking as TG in a prestrained air cooled sample. It is seen that grains are flattened due to the compressive prestrain. Some specimens had multiple cracks on the surface. A fractured indentation specimen with multiple cracks is shown in Figure 21.

C36000 showed similar trends. The results are shown in Figures 22 and 23. In this case, the dip was observed at approximately 24% true strain for the air cooled condition and at 12% true strain for the water quenched condition.

5. INDENTATION TEST FOR THE EFFECT OF TEMPERATURE

The results for the effect of temperature on the LME of air cooled C46400 are shown in Figure 24. It is observed that for low temperatures embrittlement is less and it increases with the increase in temperature. Then again the susceptibility decreases with further rise in temperature. Maximum embrittlement is obtained at 8°C.

The results of tests on air cooled C36000 are shown in Figure 25. The trend is similar to the one observed in C46400 but here maximum embrittlement occurred at 0°C.

It was also found that the temperature effects the hardness of the brass. The variation of hardness of C46400, with temperature is shown in Figure 26.
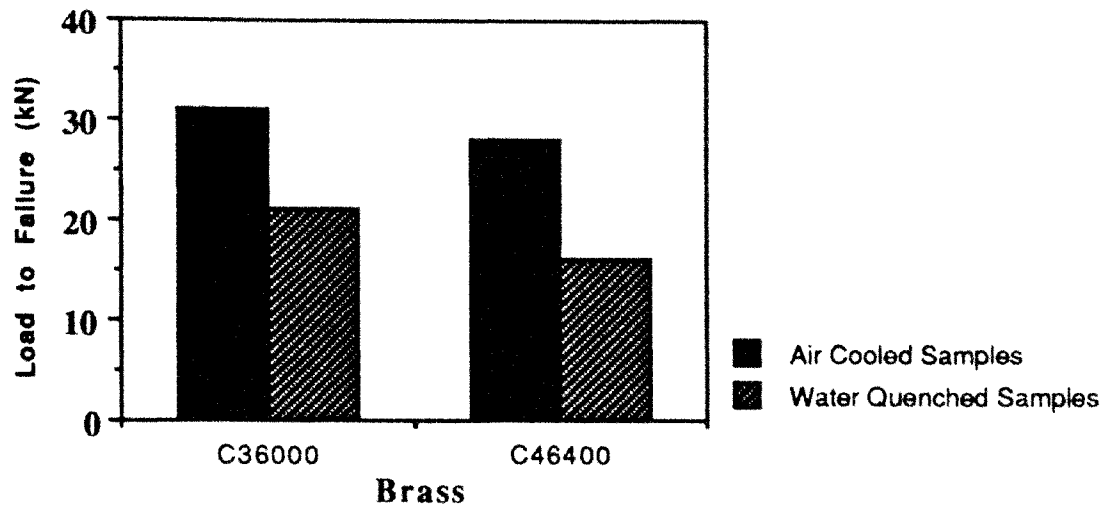
Figure 14. The plot showing the effect of heat treatment on the LME of C46400 and C36000. Note that C46400 is more embrittled than C36000. Also note that the water quenched samples are more susceptible to LME in both these alloys.
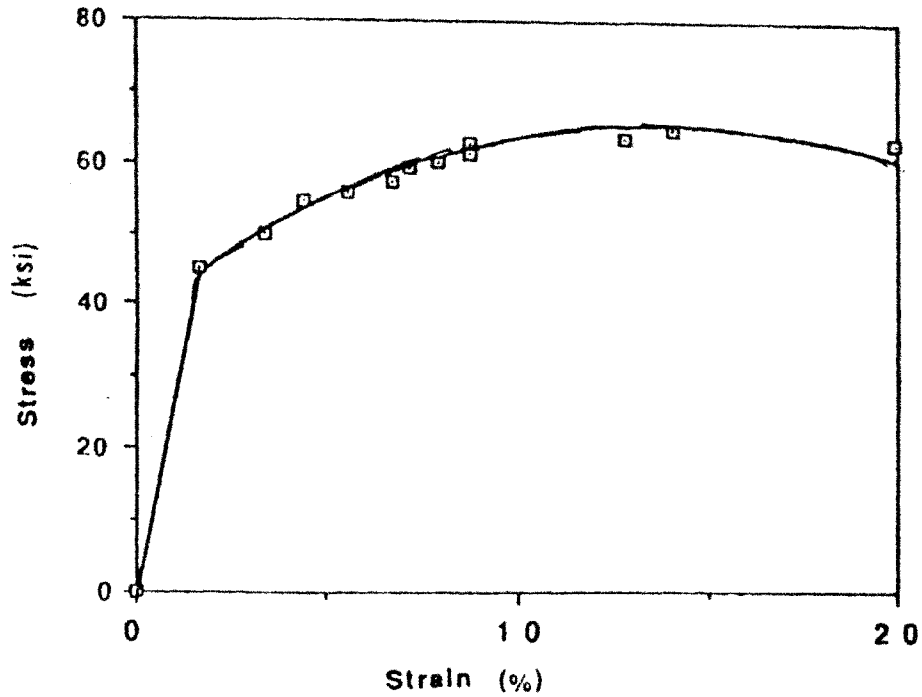
Figure 15. Stress-Strain curve for C46400 in air, obtained from the slow strain rate testing at a strain rate of 9×10^{-3}.
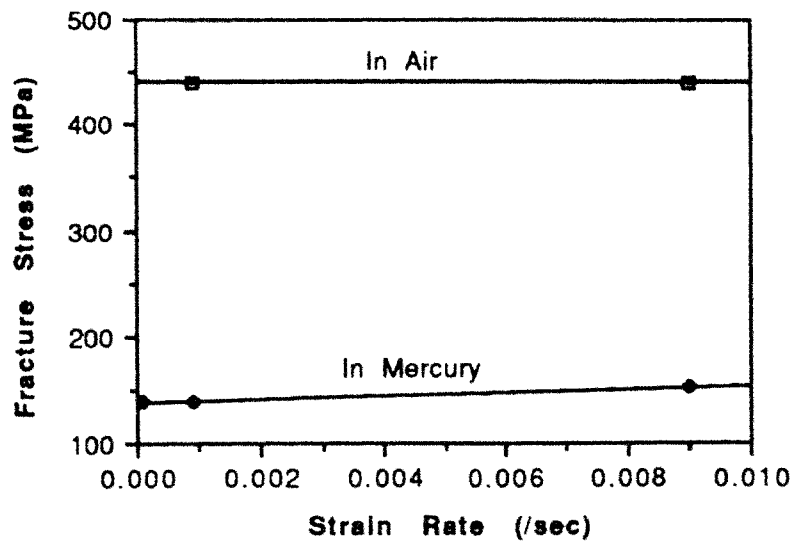
Figure 16. The plot shows that there is minimal strain rate effect on the tensile strength of C46400, when tested in air and in mercury. Also, there is approximately 65% reduction in fracture stress in mercury environment.

X 150

Figure 17. Mercury embrittlement of C46400. The mode of cracking is TG and the crack passes through the β phase.

Figure 18. Effect of prestrain on the LME of air cooled C46400. Maximum embrittlement occurs at approximately 26% prestrain. Note the reproducibility of the data.

Figure 19. Effect of prestrain on the LME of water quenched C46400. Maximum embrittlement occurs at approximately 18% true strain. Note that there is a shift in the curve towards lower cold work, when compared to the air cooled condition (Figure 18).

43
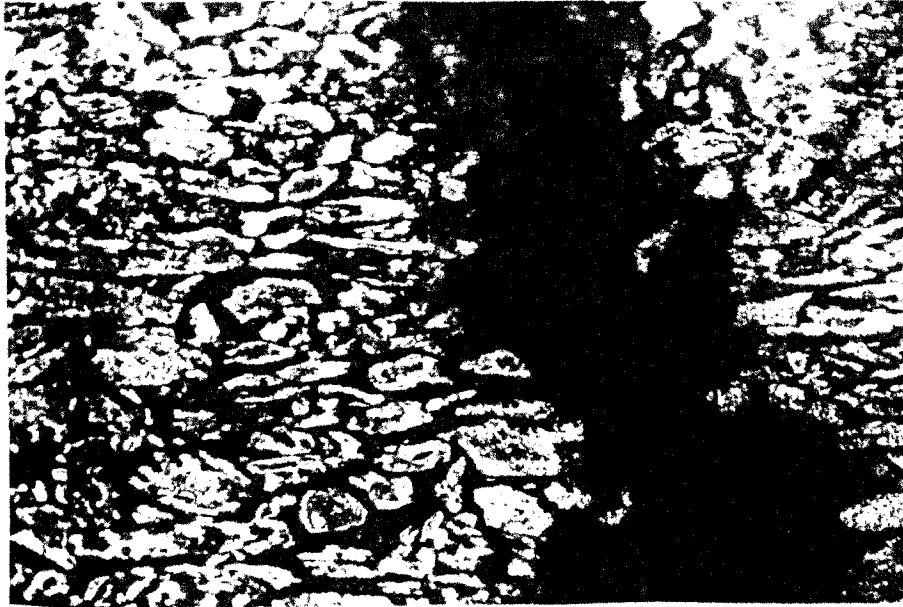
X 150

Figure 20. LME of air cooled and prestrained C46400. Cracking mode is TG through β phase. Elongated grains of α are also seen.
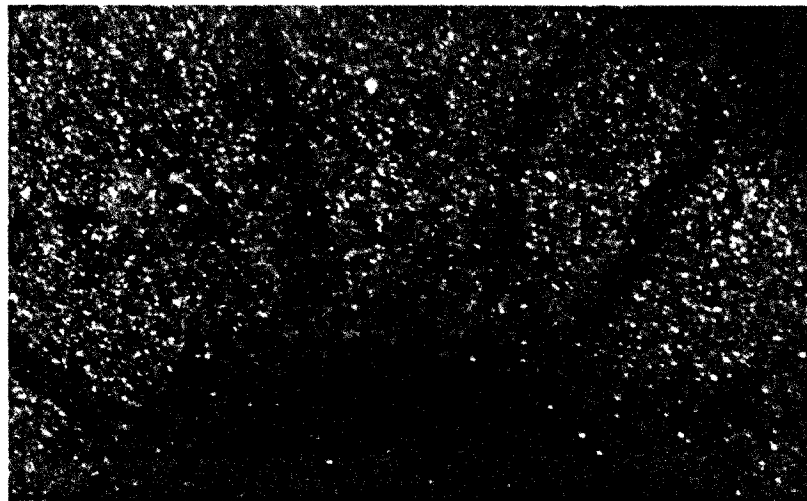
X10

Figure 21. A section of a fractured specimen with multiple cracks. Note the adherent mercury layer.

_____   _____   _____   _____

Insert Table 11 about here

_____   _____   _____   _____

In summary, the findings indicated that only 33% of west south central apparel manufacturers were involved in export of apparel. A strong need for training in developing export markets was identified by most of the west south central apparel manufacturers. Nonverbal communication behavior was reported as important by the manufacturers. As a whole, manufacturers were classified under interaction-oriented and task-oriented styles of communication.

Discussion

In general, this research supported previous studies discussed in the literature review in relation to nonverbal communication and communication styles. The findings were in agreement with the results of the study conducted by Hulbert and Capon (1972) on interpersonal communication in marketing. The results were also supported by research studies conducted on nonverbal communication by Waltman (1984) and Edwards (1991).

Employment

Majority of the manufacturers were from small companies employing 1 - 99 employees which could be the reason for lower annual employee turnover. On an average manufacturers experienced an annual turnover rate of 17%. However, this percentage may not be a true reflection of the average employee turnover rate as six small manufacturers reported zero turnover and one small manufacturer reported 100% turnover. The reason given by the manufacturer who had 100% employee turnover was "personal" such as family illness and relocation.

Manufacturers cited "lifestyle" as one of the reasons for employee turnover because the employees preferred government assistance rather than working. As suggested by Dickerson,
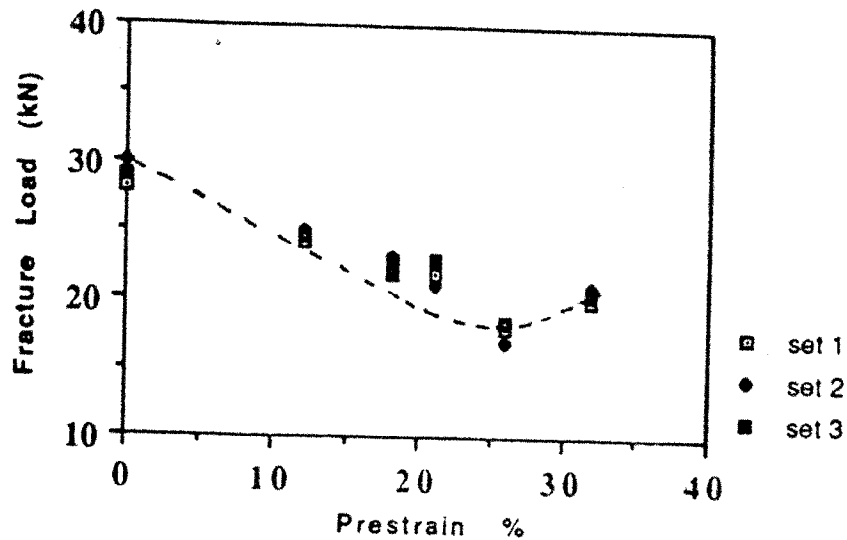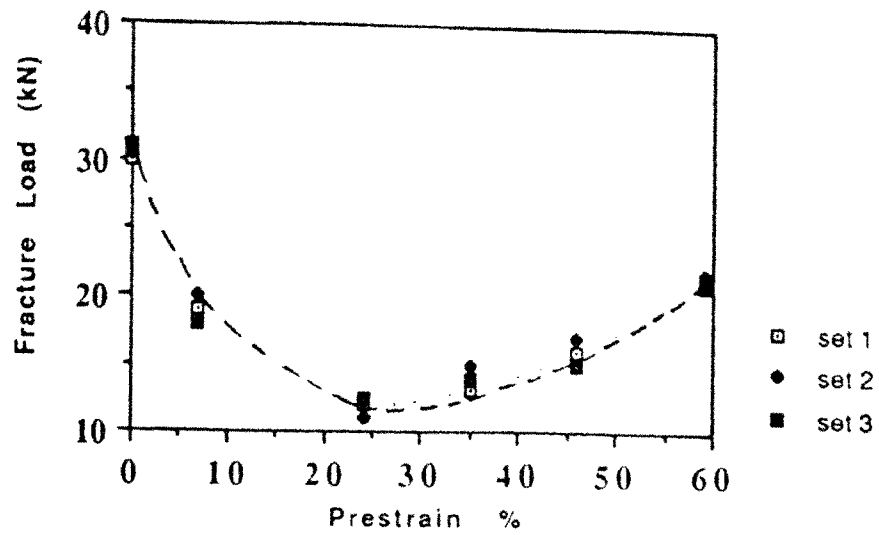
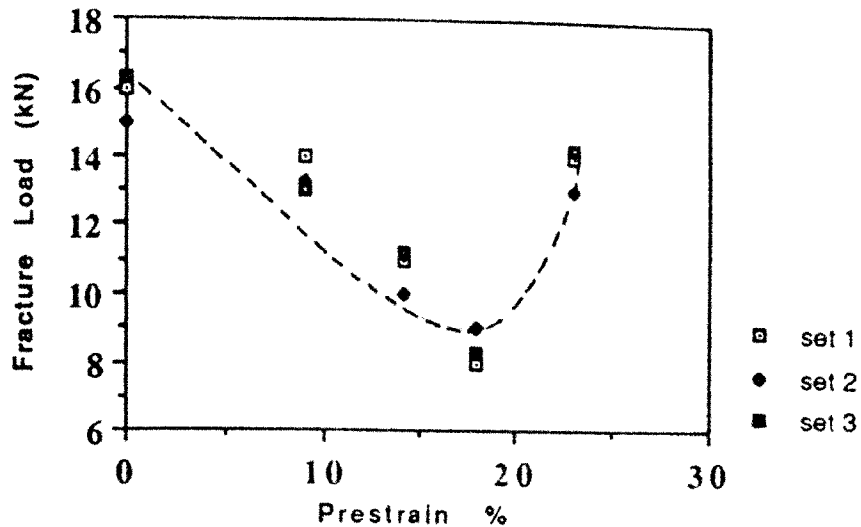Figure 22. Effect of prestrain on the LME of air cooled C36000. Maximum embrittlement occurs at approximately 24% prestrain.
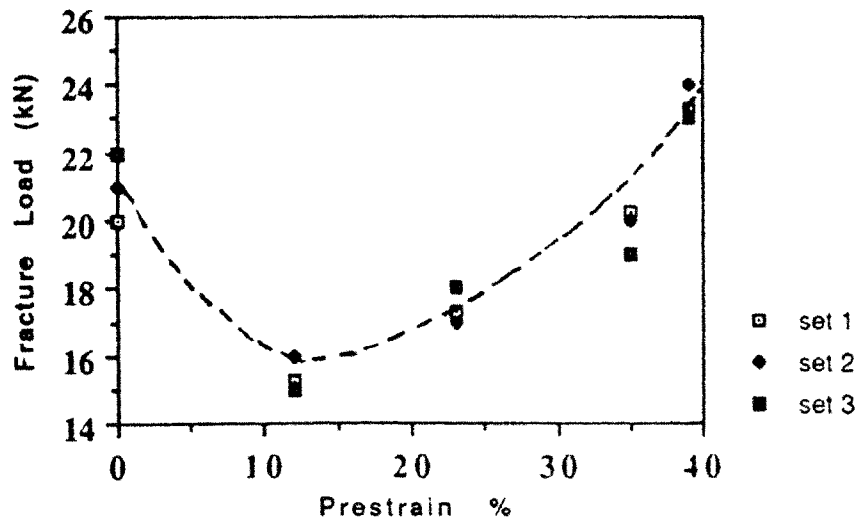
Figure 23. Effect of prestrain on the LME of water quenched C36000. Maximum embrittlement occurs at approximately 12% prestrain.

45
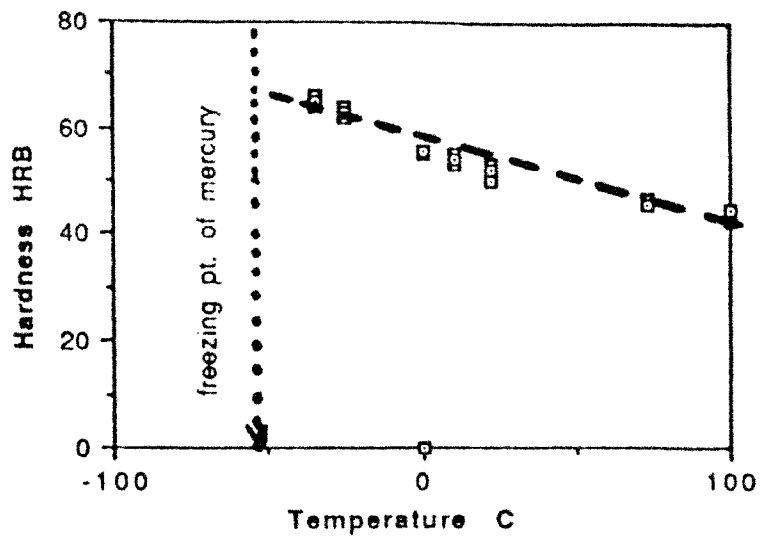
Figure 26. The plot showing the continuous decrease in the hardness of C46400 with the temperature.

CHAPTER V

DISCUSSION

1. LME OF C46400

1.1 EFFECT OF TEMPERATURE

Perhaps the most interesting feature of the results is the variation of embrittlement with temperature, as seen in Figure 24. Although embrittlement occurs at the melting point of mercury, the embrittlement is enhanced as the temperature increases up to approximately 8°C, then the embrittlement starts decreasing. An embrittlement trough is a feature of many systems. Wide embrittlement troughs have been reported in the mercury- α brass (70-30) system. It was observed by Nicholas and Rostoker (45) that the width of the trough increased with an increase in grain size in the 70-30 brass. All recovery temperatures in this alloy were well above room temperature. For grain sizes varying from 0.003 mm to 0.055 mm, they found the trough width ranging from 75°C to 160°C. But nowhere do they mention how the tests were performed at higher temperatures, and how mercury contamination of the environment was avoided. A point being that the vapor pressure of mercury will be very high at higher temperatures as shown in Table II. The occurrence of a trough with the minimum a little below room temperature, as shown in Figure 25, has not been reported for brass. Note for

Figure 24, that the experiments were repeated on different occasions and the data were reproducible.

Usually, a trough is a result of two competing processes. In this instance, the competing factors that vary with temperature may be the diffusion, fluidity, wettability, and surface tension of the mercury and the mechanical properties of the brass. As the temperature increases, the fluidity of mercury increases exponentially (62). Variation of fluidity with temperature is given by

$$\eta = (Ce^{E/RT})..(4)$$

where η = viscosity = 1/fluidity

C is a constant

T is temperature in ^{O}K

for mercury C = 0.5565 cP

E = 0.6 Kcal/mol

The fluidity of mercury at different temperatures is shown in Figure 27. Note that there is about a 30% increase over the temperature range -38 to 25°C.

The self diffusion rates in solids and liquids always increases with increase in temperature. The data for mercury are shown in Figure 28 (63). Note that the rates are of the order of $10^{-5}cm^2/sec$. Again there is about a 30% increase between -35 and 20°C. However, such a low self diffusion rate cannot explain the high crack propagation rates observed in the case of LME. So the
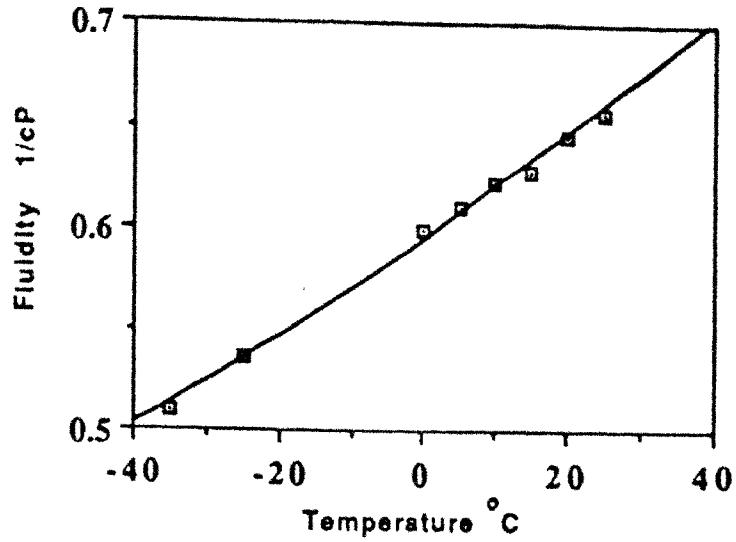
Figure 27. Plot showing the increase in the fluidity of mercury with the increase in temperature.(data points obtained using eq. 4) (56).
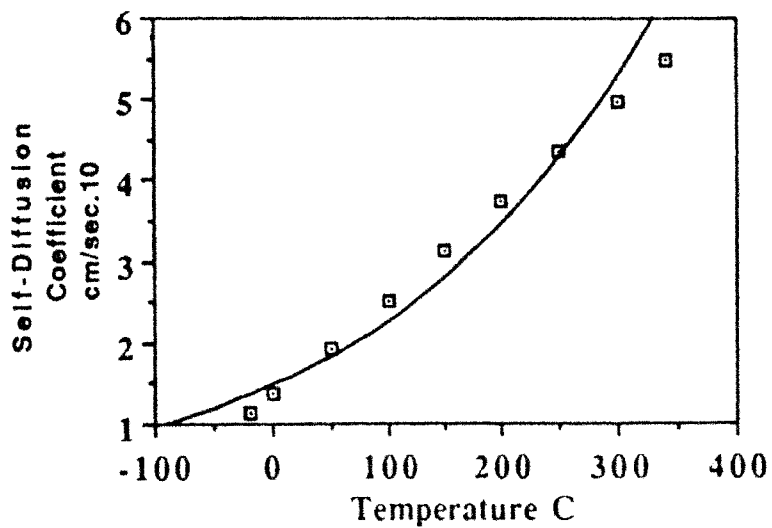
Figure 28. Plot showing the exponential increase in the self diffusion of mercury with increase in temperature (graph based on the data obtained from ref. 57).

transportation of mercury occurs by some other mechanism, rather than bulk diffusion. However, to explain the high crack propagating rates, it is suggested by Westwood and Kamdar (64) that the transport to a propagating crack tip occurs by a monolayer process like by mercury atoms over mercury atoms, rather than mercury atoms over zinc atoms. While the actual value of the activation energy Q for the second monolayer diffusion of mercury on mercury has not been determined, Q for cesium is approximately 0.1 eV and D_O is approximately 10^{-2} cm^2 s^{-1} at about 30°C (65). These values suggest that second monolayer diffusion of liquid in liquid phase should be capable of maintaining a sufficient supply of liquid metal atoms at the crack tip to explain observed rates of crack propagation.

The surface tension of liquids always decreases with the increase in temperature. The surface tension of the mercury at 20°C is 37.5 N/m. While the surface tension of mercury at other temperatures have not been determined, the surface tension of water at different temperatures is shown in Figure 29 (66). Foregoing factors will all facilitate the transportation of mercury to a crack tip, therefore should favor an increase in embrittlement with an increase in temperature.

However, the mechanical properties of metals vary with temperature. In this study, hardness was used as a convenient means of illustrating the change in mechanical properties with temperature. Hardness is a measure of the resistance to the plastic deformation so relates to the constrained yield strength of a material. It was found that the hardness of brass decreases with the increase in temperature (Figure 26). So, it can be inferred that the yield strength decreases proportionally with the increase in temperature.

51
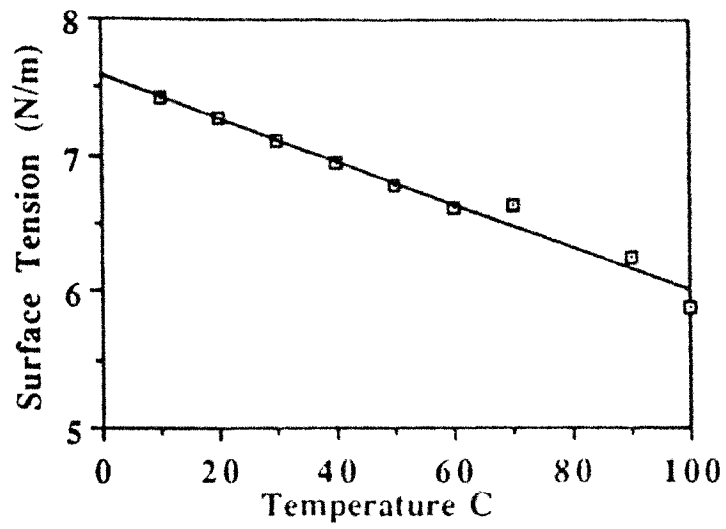
Figure 29. Plot showing the decrease in the surface tension of water with the increase in temperature (66).

In FCC metals, the tensile strength decreases far more rapidly with temperature increase than does the yield strength (Figure 30). The difference between yield strength and tensile strength is a measure of the strain hardening ability of the metal, hence the equation

$$\sigma = k\varepsilon^n \quad \dots\dots\dots\dots\dots\dots\dots\dots\dots\dots\dots\dots\dots\dots\dots(5)$$

where σ is stress, ε is strain and k and n are constants.. So, there is a decrease in 'n' with the increase in temperature. This decrease in 'n' signifies more ready cross slip, which would facilitate plastic deformation at the crack tip, which would result in the blunting of the crack tip, rather than the propagation of a brittle crack.

In the case of BCC metals, the yield strength is higher but n is lower because of the ease of cross slip resulting from the absence of partial dislocations. The yield strength increases very rapidly at low temperatures, resulting in the well known ductile-to brittle transition (Figure 31). At higher temperatures, the yield strength does approach the tensile strength, so plasticity and crack tip blunting are favored

The foregoing is pertinent because alloy C46400 is a two phase FCC-BCC α–β brass. Figure 32 illustrates the variation of tensile strength and yield strength with temperature for α–β forging brass akin to C46400 (67). From the Figure 32, it can be seen that the plot resembles that of an FCC metal, thus FCC phase dominates the mechanical properties. But it must be remembered that the cracking is through BCC β phase. The FCC phase would be softer and yield at a lower stress, so perhaps give rise to stress concentration at the α–β interface that will trigger the brittle fracture in the β phase.

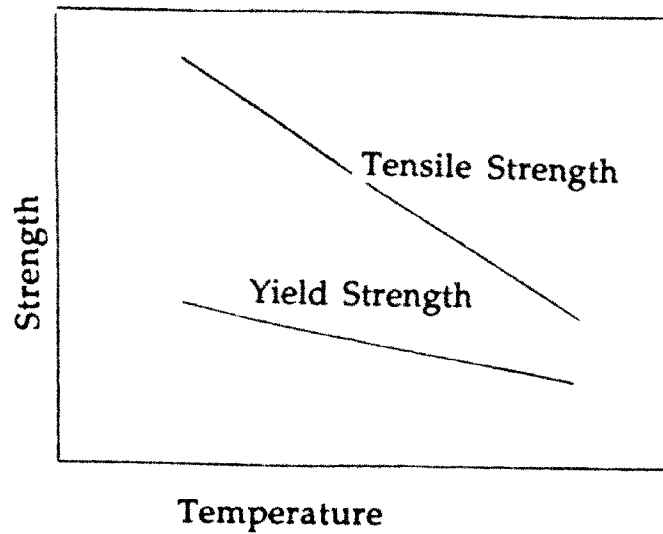Figure 30. Schematic diagram showing the effect of temperature on the yield and tensile strength of FCC metals.
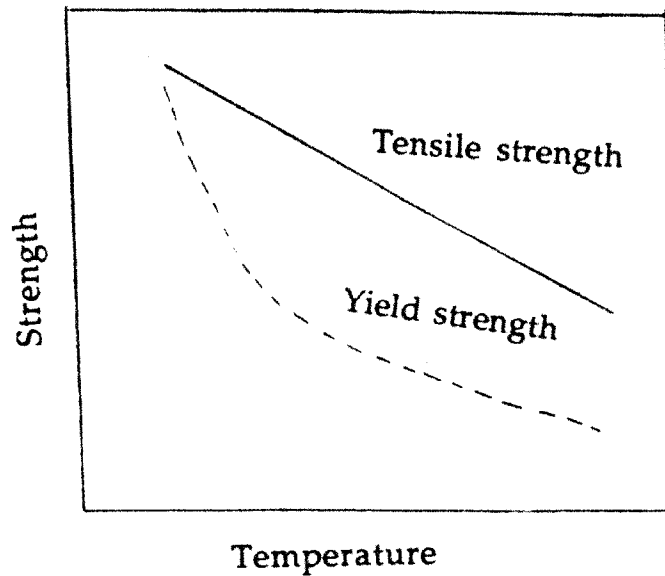
Figure 31. Schematic diagram showing the effect of temperature on the yield and tensile strength of BCC metals.

Because of these opposing factors, we observe an embrittlement trough. The effect of these factors on embrittlement is schematically shown in Figure 33.

For a brittle fracture to occur, liquid mercury must be present at the crack tip. There are two possibilities: 1. Crack initiation leads to failure and 2. Crack initiation does not lead to failure.

For the first case, it is required that liquid metal be continuously present at the propagating crack tip (Figure 34). Fluid mechanics of the system controls the rate at which the bulk liquid metal travels to the vicinity of the crack tip. Rostoker et al. (12) suggested that a driving force of 10^5 atm would be required for "bulk" liquid metal present at an atomically sharp crack tip. Capillarity effects could provide "negative" pressure of order 10^4-10^5 atm, which would pull the liquid metal into very small cracks, aiding transport to the tip.

In the second case, mercury does not reach the sharp crack tip, maybe because of the less reactivity (Figure 35). The only condition in which it reaches the crack tip is when the crack tip is blunted. Since blunting is a stress dependent process, crack initiation does not immediately lead to failure.

1.2 EFFECT OF STRAIN RATE

Even though alloy C46400 is a two phase alloy, its properties are dominated by a phase which is FCC and in general FCC structures are not strain rate sensitive in air. It was found from the experiments that it was not strain rate sensitive in the mercury environment, also. But, there was considerable reduction in fracture stress when the tests were done in mercury,
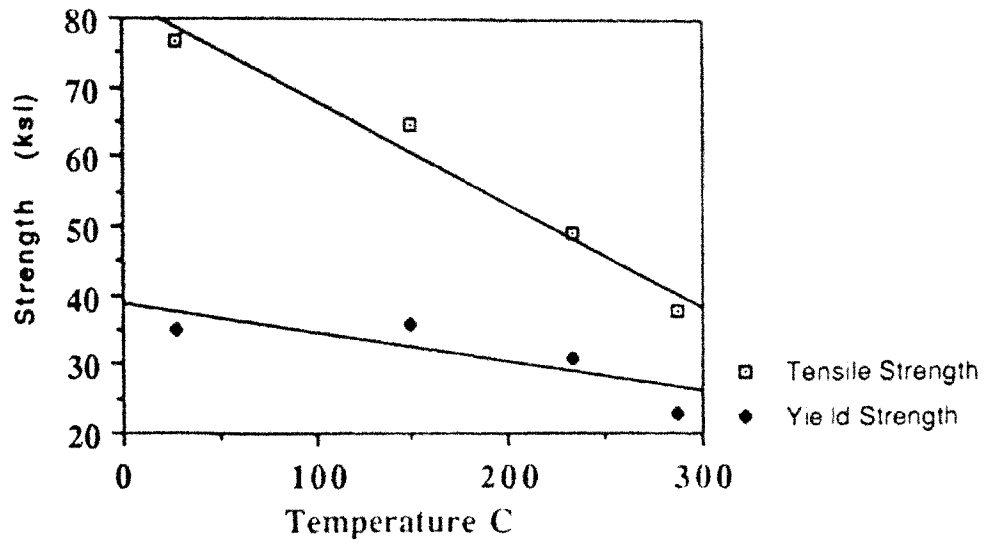
Figure 32. Effect of temperature on the yield and tensile strength of C37000 (data obtained from ref. 67). Note that the plot resembles the behavior of an FCC metal (Figure 30).
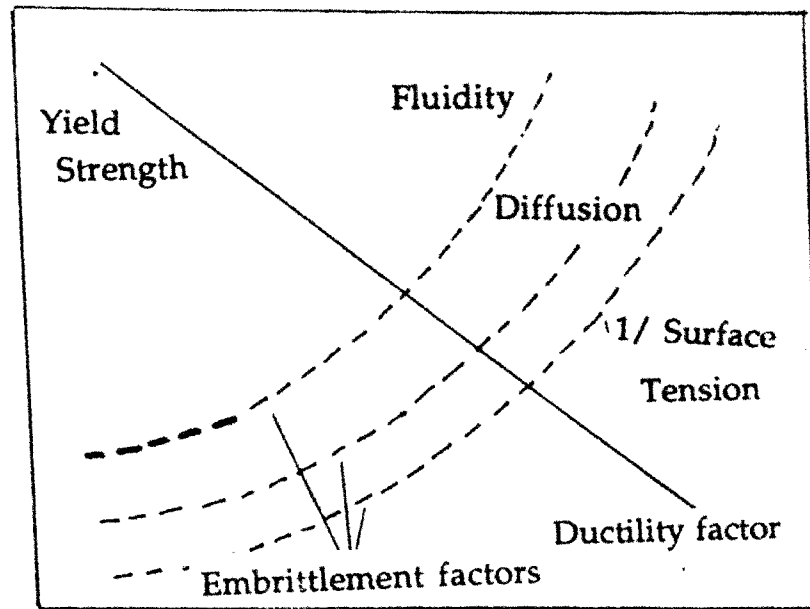
Figure 33. Schematic diagram showing the effect of various factors effecting LME.
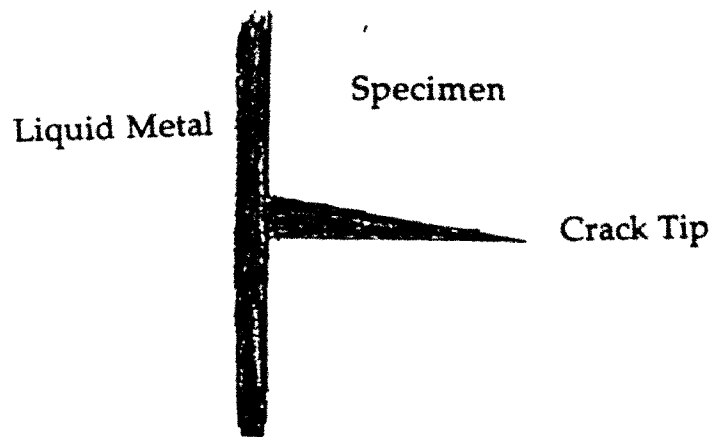
Figure 34. Condition for the case when the crack initiation leads to failure. In this case, mercury reaches the crack tip.
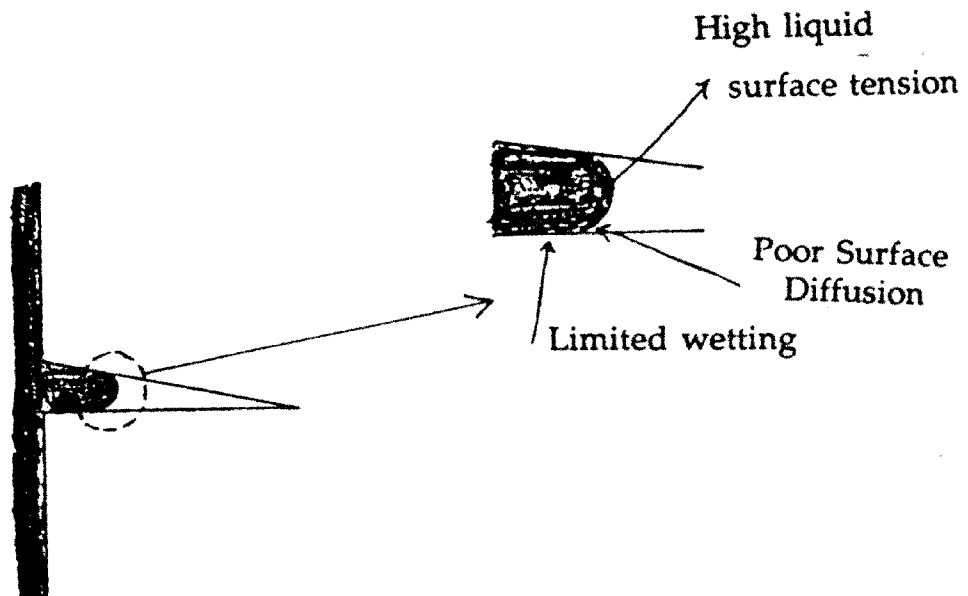
Figure 35. Condition for the case when crack initiation does not lead to failure. In this case, mercury does not reach the crack tip because of high liquid surface tension and poor surface diffusion.
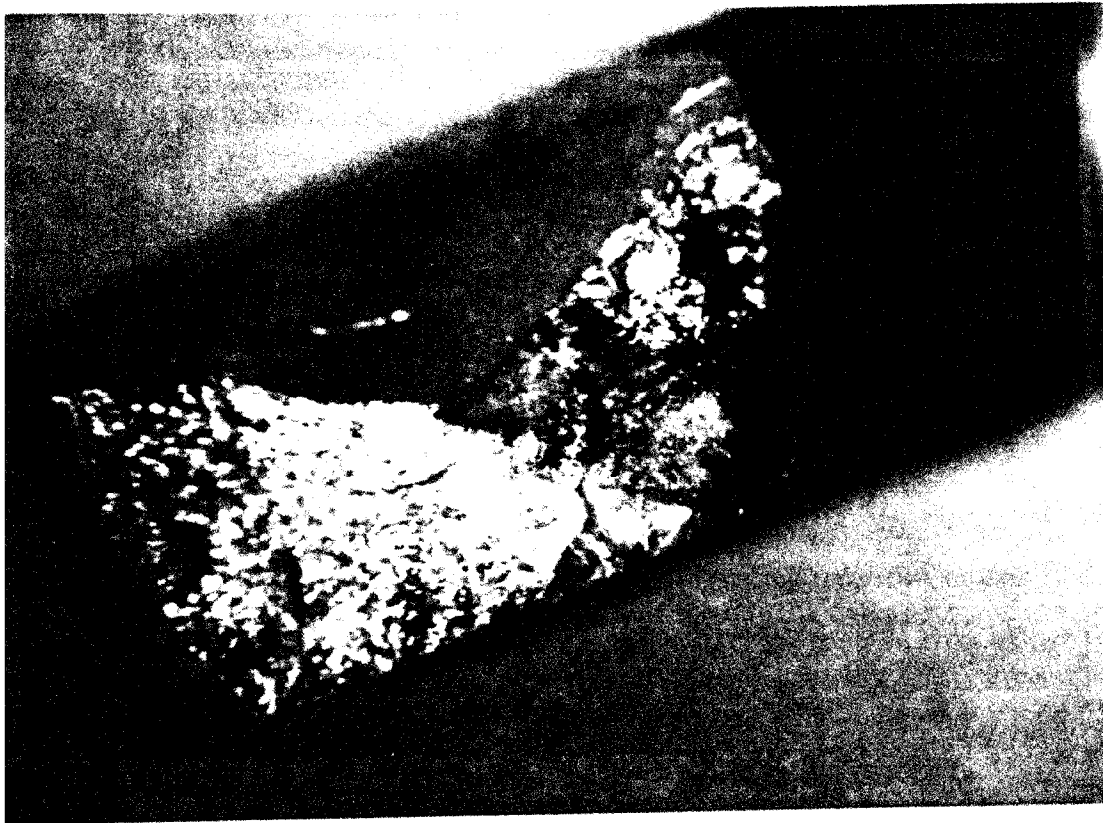
X 10

Figure 36. Fractured specimen of the brass showing the mercury adhering to the fractured surface. It implies that the mercury is in intimate contact with the brass and ready to react as soon as the critical strain threshold is reached.

as compared to the results of the tests done in air. Samples failed below the yield stress in mercury.

A strain sensitivity when tested in liquid mercury would imply an incubation period before crack initiation, a delay in the mercury reaching the crack tip and/or a time dependent reaction at the crack tip. But, it was observed that in slow strain rate tests over a given strain rate range as well as indentation tests, crack initiation led to failure (case 1). Moreover the fractured surface was fully covered with mercury (Figure 36). Therefore the ability of the liquid mercury to reach and react at the crack tip was not a limitation. It implies that the mercury is in intimate contact with the brass and ready to react as the soon as the critical strain threshold is reached. Hence, it is inferred that the LME of brass is influenced by factors that effect the crack initiation rather than the crack propagation.

1.3 EFFECT OF HEAT TREATMENT

It was observed (Figure 14) that the water quenched specimens were more susceptible to embrittlement by mercury than air cooled specimens. The microstructure revealed that water quenched samples had more β than air cooled ones. In both the cases, the crack was TG and passed through the β phase.

This can be explained using the phase diagram of Cu-Zn (Figure 37). At 800°C, only the β phase exists and when a sample is water quenched, only small amount of α precipitates out. This results in a microstructure that is mostly β at room temperature. In the case of air cooled samples, much more α precipitates out, decreasing the amount of β at room temperature.

β is a BCC structure and hence stronger and less ductile than the α phase, which is an FCC structure (68). Also, it has been observed that the increase in zinc content, which results in increased β phase, increases the susceptibility to LME (28, 29, 30). From these observations, we can conclude that the β phase is more susceptible to embrittlement. Therefore the cracking was mainly through β phase even though there is mention of cracking through α phase under different conditions.

1.4 EFFECT OF COLD WORK

Here again we observe an embrittlement trough. Increased cold work results in an increased dislocation density which act as crack nucleation sites (43). Also, as cold work increases, yield strength increases. This increased yield strength prevents the crack tip blunting and thus favors embrittlement. But susceptibility starts diminishing from about 27% true strain for air cooled condition and from about 18% for water quenched condition. This behavior is similar to the results obtained by Rinnavatore (36) on α brass, who observed maximum embrittlement at 22% true strain. However, he had observed IG cracking for material rolled between 0 and 50% reduction and TG for material rolled to 75 and 95% reduction. He hypothesized that the embrittlement decreases across because of the lack of transverse grain boundaries. A similar argument could be employed in here that the cold work enhances the effectiveness of the α phase as a crack propagation barriers, by flattening the grains. Since embrittlement is a localized phenomenon, it can be argued that the microstructure is full of high energy sites through the high dislocation density and that crack blunting becomes easier because of readier cross slip.
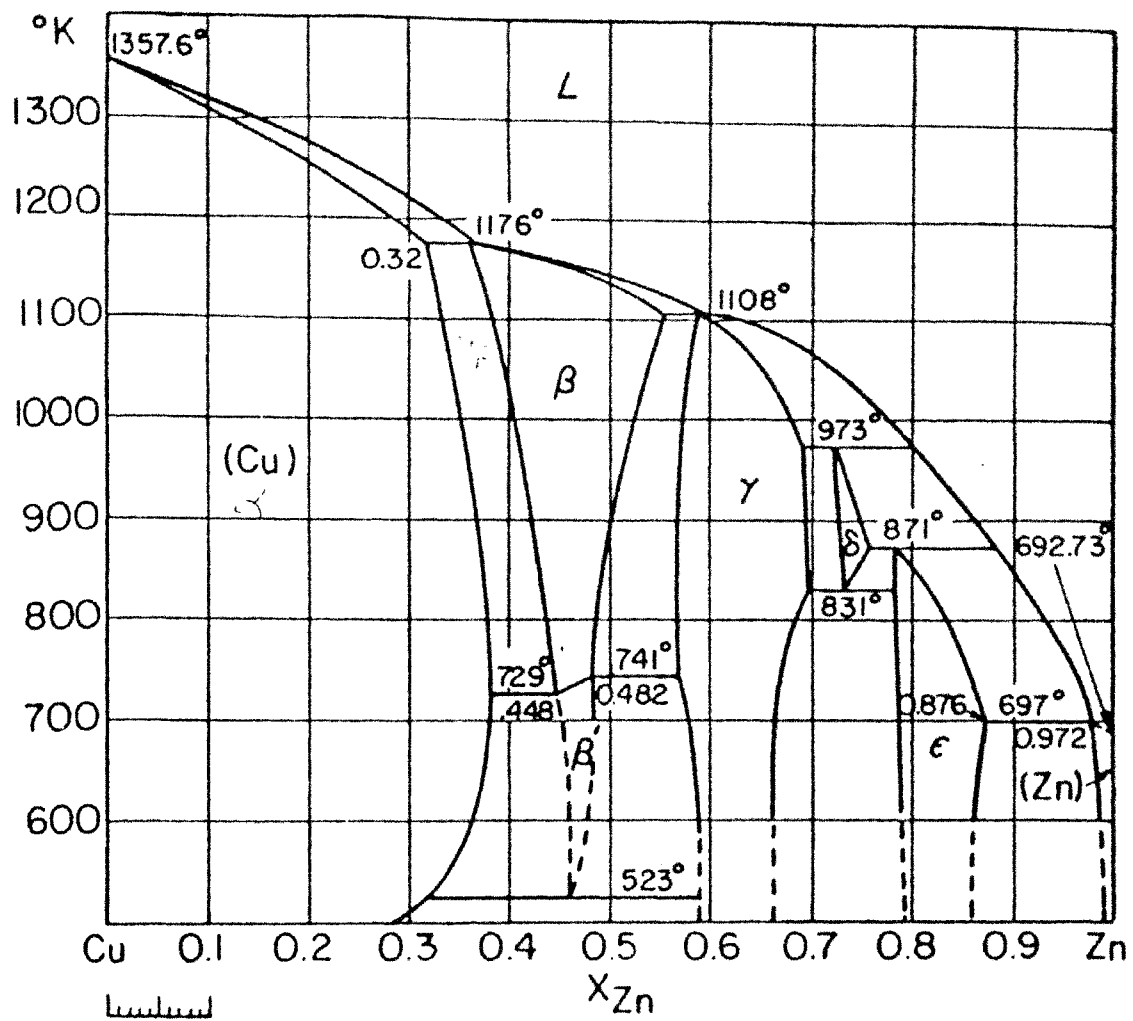
Figure 37. Phase diagram of Cu-Zn (69).

62

The shift in the curve for the water quenched condition towards lower cold work is because of the presence of more β in this condition as compared to air cooled ones.

2. COMPARISON TO C36000

In this leaded brass, lead appears to be an inert constituent as regards embrittlement. A small amount of β phase is present in the microstructure. Therefore, based on the observations with the C46400 brass, it would be anticipated that the same trends would occur; cracking through the β phase and 'U' shaped curves versus prestrain and temperature. The lower β content should signify a lower degree of embrittlement. This study and the one conducted by Pidathala (42) show that these events do occur (Figures 22, 23, and 25).

3. COMPARISON TO ALPHA BRASSES

Brasses containing less than about 30% zinc are single phase. While they were not part of this study, it should be noted that embrittlement by liquid mercury still occurs, either through the α phase or IG. The latter is likely an impurity effect, for embrittlement in steels, stainless steels and nickel base alloys can be IG when 'sensitized'. Another comparison mentioned in chapter 2, is that SCC can be through the α phase or IG, depending on the pH. In the α-β brasses, SCC is TG through α and β (29). A difference between SCC and LME is that the former is strain rate sensitive because of the rate process of transportation.

4. COMPARISON TO COPPER

C11000 is most resistant to LME, when compared to C36000 and C46400 (32, 33, 34). Embrittlement is so much less in some cases that some of the earliest experimentalists even claimed that it was not embrittled by mercury (7, 24).

Study by Peevy (36) has demonstrated that C11000 is embrittled by liquid mercury. But in this study, it was found that they were not embrittled under indentation tests. This is because their embrittlement is strain rate sensitive. Since wetting difficulties were also noted, the inference is that it is the wetting stage that is responsible for the time delay.

5. COMPARISON TO ALLOY N04400

This solid solution alloy is approximately 66% Ni-34% Cu. It is extensively used in the oil industry, for example, for fittings to resist corrosion. Its resistance to LME by mercury has been studied extensively in this lab (1, 2). The alloy has proved to be highly susceptible to LME, giving IG fracture. The feature of interest is that the embrittlement, as in copper, is strain rate sensitive and crack initiation does not lead to failure. The alloy is not readily wetted by mercury and small spheres of mercury are often found on completely dewetted fracture surfaces. The inference is that the embrittlement is controlled by the ability of mercury to wet the alloy and to reach the crack tip. It is the opposite situation to that of brass.

6. COMPARISON TO AGE-HARDENING ALUMINUM ALLOYS

LME of age-hardened aluminum alloys- Al2024, Al7075 and Al6061 have been recently studied in this lab (3, 4, 5). Aluminum being highly reactive to the environment, requires extremely low free energy for the formation of Al_2O_3 and this makes the wetting difficult as compared to the wetting of brass. The problem of wetting was solved by etching the surface with 10% HF, which is capable of breaking the oxide layer. Like brass, they were also not found to be strain rate sensitive. The crack initiation led to failure

There is continuous decrease in embrittlement severity with the increase in temperature as compared to a dip in case of brass. There was decrease in embrittlement of brass at very low temperatures because of the decrease in the wetting. But in case of aluminum alloys, wetting remained same at all the test temperatures, and the only influencing factor was the yield strength.

CHAPTER VI

CONCLUSIONS

The findings of this report are:

1. In case of C46400 or C36000 brass, crack initiation always led to immediate failure because of the thorough wetting of the surface with the mercury. Hence, the liquid metal embrittlement of brass is influenced by the factors that effect the crack initiation rather than the crack propagation. For this reason, embrittlement of brass is not strain rate sensitive over the strain rates tested.

2. An embrittlement trough is observed with the variation of temperature, maximum embrittlement occurring slightly below room temperature. This is presumed because of the increase in the fluidity, increase in the diffusion rate and the decrease in the surface tension of mercury with the increase in temperature favors embrittlement with the increase in temperature, whereas, decrease in the yield strength of brass with the increase in temperature favors recovery.

3. The increase in the yield strength with the increase in the prior cold work favors embrittlement, whereas the increase in the dislocation density and the flattening of the α grains with the increase in the prior cold work favors recovery. Hence, an embrittlement trough is observed with the variation of the prior cold work.

4. If a designer has to choose between C36000 and C46400, he should select either C36000 with 0% cold work or choose C46400 with very high degree of cold work (> 75%) in order to get maximum strength in mercury environment.

5. Since cracking is transgranular (TG) through the β phase, factors which tend to decrease the β phase, will increase the resistance to embrittlement. Therefore, air cooled samples are more resistant than water quenched samples. Also, C36000, which has less amount of β, shows similar behavior except that it is less embrittled than C46400.

6. As contrast to brass, in C11000 and N04400, crack initiation does not lead to failure because of the wetting problems, and hence they are strain rate sensitive. This is believed to be related to the difficulties in wetting. But like in brass, crack initiation leads to failure in case of age-hardening aluminum alloys, and hence no strain rate sensitivity is observed in these alloys.

7. Any alloy, in which liquid metal readily wets the surface, will show no strain rate sensitivity. In these alloys, crack initiation would lead to failure. Moreover, they would be embrittled by indentation tests. On the other hand, alloys in which there is wetting problem with the liquid metal, crack initiation would not lead to failure, and their embrittlement would be strain rate sensitive. Also, they would not be embrittled by indentation tests.

REFERENCES

1. Price, C. E. and Good, J. K. <u>Trans ASME,</u> Vol. 106, p 184 (1984).

2. Price, C. E., Traylor, L. B. <u>J. Eng. Mets. Tech,</u> Vol. 108, p. 31 (1986)

3. Kotha, S. Masters Report, Oklahoma State University, Stillwater, Collage of Mechanical and Aerospace Engineering. (1993).

4. Pannerselvem, B. Masters Report, Oklahoma State University, Stillwater, Collage of Mechanical and Aerospace Engineering. (1993).

5. Mogheese, S., Masters Report, Oklahoma State University, Stillwater, Collage of Mechanical and Aerospace Engineering. (1993).

6. Gynadesikan, R.,Masters Report, Oklahoma State University, Stillwater, Collage of Mechanical and Aerospace Engineering. (1993).

7. Mattsson, E. <u>Elecrochemica Acta,</u> Vol. 3, p. 279 (1961).

8. Wedler, G. <u>Chemisorption: An Experimental Approach,</u> Butherworths Inc., Boston, p. 199 (1976).

9. <u>Associated Press News Realease,</u> SNP, 8-20-1993.

10. Kamdar, M. H. <u>Metals Handbook,</u> Vol. 11, 9th Edition, p.225 (1986).

11. Johnson, W. H. <u>Proc. Royal Soc. Lon.,</u> Vol. 23, p. 168 (1874) republished in <u>Hydrogen Damge,</u> C. D. Beachem, ed. ASM, Metals Park, Ohio, p.1 (1977).

12. Rostoker, W.; Mc Caughy, J. M.; and Markus, H. <u>Embrittlement by Liquid Metals,</u> Rreinhold Publishing Corp., New York (1960).

13. Kamdar, M. H. <u>Metals Handbook,</u> Vol. 13, 9th Edition, p. 171 (1986).

14. Wheeler, D. A; Hoagland, R. G; and Hirth, J. P Corrosion, Vol. 45, No. 3, p. 207 (1989).

15. Moore, H; Beckinsale, S; and Mallinson, C. E. J. Inst. Metals, Vol. 25, pp 35-126 (1921).

16. Kamdar, M. H. Embrittlement of Engineering Alloys, Vol. 25, p. 361 (1983).

17. Pickens, J. R.; Precht, W.; and Westwood, A. R. C. J. Mater. Sci., Vol. 18 pp. 1872-1880 (1983).

18. Wilson, T. C.; Edmunds, G.; Anderson, E. A.; and Pierce, W. H. Symposium on Stress Corrosion Cracking of Metals, ASTM / AIME: Philadelphia, p. 173 (1944).

19. Stoloff, N. S. Environment-Sensitive Fracture of Engineering Materials, Z. A. Foroulis, ed., AIME: Warrendale, Pennsylvania, pp. 486-518 (1979).

20. Stoloff, N. S. "Solid and Liquid Metal Embrittlement." Presented at the NATO Advanced Study of Atomistics of Fracture, Corosica (1981).

21. Stoloff, N. S. Acta Met., Vol. 11, p. 251 (1963).

22. Robertson, N. J. Met. Trans., p. 2607 (1970).

23. Krishtal, M. A. Sov. Phy. Dolk., Vol. 15, p. 159 (1975).

24. Lynch, S. P. Scripta Met., Vol. 13, p. 1051 (1979).

25. Lynch, S. P. Acta Met., Vol. 29, p. 325 (1981).

26. Westwood, A. R. C., and Latinson, R. M. "Corrosion by Liquid Metals.", TMS-AIME, Vol. 212, p. 192 (1958).

27. Kamdar, M. H. "Embrittlement by Liquid Metals.", Prog. Mat. Sci., Vol. 15, p. 289 (1973).

28. Edmunds, G.; Anderson, E. A.; and Waring, R. K. Symposium on Stress Corrosion Cracking of Metals, ASTM / AIME: Philadelphia, p. 7 (1944).

29. Edmunds, G. Symposium on Stress Corrosion Cracking of Metals, ASTM / AIME: Philadelphia, p.67 (1944).

30. Whitaker, M. E. Metallurgia, Vol. 39, p. 21 (Nov. 1948).

31. Robertson J. of Met. Trans AIME, Vol. 3, p.1190 (1951).

32. Shunk, and Worke, Scripta Met, Vol. 8, p. 519 (1974).

33. Stoloff, N. S., Davies, R. G., and Johnston, T. L. Environment Sensitive Mechanical Behavior, New York: Gorden and Beach, Science Publishers, Inc., pp. 613-655 (1966).

34. Tiner, N. A. Trans. Met. Soc. AIME, Vol. 221, p. 261 (1961).

35. Rosenberg, R. and Cadoff, I. Fracture of Solids, New York, John Wiley, P. 607 (1963).

36. Peevy, G. R. Masters Report, Oklahoma State University, Stillwater, Collage of Mechanical and Aerospace Engineering. (1984).

37. Greenwood, J. N. J. Inst. Metals, Vol. 81, No. 7, pp. 177-178 (1953).

38. Cotrell, A. H. TMS-AIME, Vol. 5 p.192 (1958).

39. Perech, N. J. Prog. Met. Phy., Vol. 5, p. 1 (1954)

40. Gorden, P., and Henry, H. Metallurgical Trans., Vol. 13A, pp. 457-472 (1982).

41. Rinnovetore, J. V; McCaughy, J; and Markus, J. D Trans ASM, Vol. 61, p.321 (1964).

42. Pidathala, M. P. Masters Report, Oklahoma State University, Stillwater, Collage of Mechanical and Aerospace Engineering. (1993).

43. Rinnovatore, J. V; Corrie, and J. D; Meakin, J.D Trans. ASM, Vol. 61, p. 321 (1968).

44. Nicholas, M. G. J. Met. Sci., Vol.14 pp 1-18 (1960).

29. Edmunds, G. Symposium on Stress Corrosion Cracking of Metals, ASTM / AIME: Philadelphia, p.67 (1944).

30. Whitaker, M. E. Metallurgia, Vol. 39, p. 21 (Nov. 1948).

31. Robertson J. of Met. Trans AIME, Vol. 3, p.1190 (1951).

32. Shunk, and Worke, Scripta Met, Vol. 8, p. 519 (1974).

33. Stoloff, N. S., Davies, R. G., and Johnston, T. L. Environment Sensitive Mechanical Behavior, New York: Gorden and Beach, Science Publishers, Inc., pp. 613-655 (1966).

34. Tiner, N. A. Trans. Met. Soc. AIME, Vol. 221, p. 261 (1961).

35. Rosenberg, R. and Cadoff, I. Fracture of Solids, New York, John Wiley, P. 607 (1963).

36. Peevy, G. R. Masters Report, Oklahoma State University, Stillwater, Collage of Mechanical and Aerospace Engineering. (1984).

37. Greenwood, J. N. J. Inst. Metals, Vol. 81, No. 7, pp. 177-178 (1953).

38. Cotrell, A. H. TMS-AIME, Vol. 5 p.192 (1958).

39. Perech, N. J. Prog. Met. Phy., Vol. 5, p. 1 (1954)

40. Gorden, P., and Henry, H. Metallurgical Trans., Vol. 13A, pp. 457-472 (1982).

41. Rinnovetore, J. V; McCaughy, J; and Markus, J. D Trans ASM, Vol. 61, p.321 (1964).

42. Pidathala, M. P. Masters Report, Oklahoma State University, Stillwater, Collage of Mechanical and Aerospace Engineering. (1993).

43. Rinnovatore, J. V; Corrie, and J. D; Meakin, J.D Trans. ASM, Vol. 61, p. 321 (1968).

44. Nicholas, M. G. J. Met. Sci., Vol.14 pp 1-18 (1960).

45. Nicholas, H., and Rostoker, W., Acta Met., Vol. 8, p 842 (1960).

46. Morris, A. Trans. Am. Inst. Min. and Met. Engrs., Vol. 18, p.153 (1918).

47. Suzuki, Y., and Hisamatsu, Y. Corrosion Science, Vol. 21, pp. 353-368 (1981).

48. Bassett, W. H. Proc. ASTM, Vol. 18, p.153 (1918).

49. Moore, h.; Beckinsale, S.; and Mallinson, C. E. J. Inst. Metals, Vol. 25, pp. 35-152 (1921).

50. Hartley, H. J. J. Inst. Metals, Vol. 37, pp. 193-214 (1927).

51. Genders, R. J. Inst. Metals, Vol. 37, p. 217 (1927).

52. Discussion by Maurice Cook of paper on: "The effects of Two Years' Atmospheric Exposure on the Breaking Load of Hard Drawn Non-Ferrous Wires.", by Hudson, J. C. J. Inst. Metals, Vol. 44, pp. 426-428 (1930).

53. Pugh, E. N.; Montague, W. G.; and Westwood, A. R. C. Corros. Sci. Vol. 6, p. 345 (1966).

54. Thompson, D. H., and Tracy, A. W. Trans AIME, Vol. 185, p.100 (1949).

55. Pugh, E. N.; Craig, J. V.; and Montague, W. G. Trans. ASM , Vol. 61, p. 468 (1968).

56. Uligh, H. H., and Duquette, D. J. Corros. Sci., Vol. 9, p. 557 (1969).

57. Escalante, E., and Kruger, J. J. Electrochem. Soc., Vol. 118, p. 1062 (1971).

58. Takano, M. and Shimodaira, S. Trans. Jpn. Inst. Met., Vol. 7, p. 193 (1966).

59. Metals Handbook, Vol.2, "Properties and Selection: Non Ferrous Alloys and Special Purpose Materials ", 10th Edition, p 265 (1990).

60. Metallography Principles and Procedures, Leco Corporation, p.35 (1977).

61. Carasso, J. I., <u>Vapour Pressure of the Elements</u>, Academic Press, New York, p. 226 (1963).

62. Beer, S. Z., <u>Liquid Metals-Chemestry and Physics</u>, Marcel Dekker, Inc., New York, p. 456 (1972).

63. Ottar, B., <u>Self-Diffusion and Fluidity in Liquids</u>, Oslo University Press, Oslo, p.127 (1958).

64. Westwood, A. R. C., and Kamdar, M. H., <u>Phil. Mag.</u>, Vol. 8, p. 787 (1963).

65. Johnson, T. L; Davies, R. G; and Stollof, N. S , <u>Phil. Mag.</u> Vol. 12, p. 305 (1965).

66. Gehart, P. M., Gross, R. J. Fundamentals of Fluid Mechanics, Addison-Wesley Publishing Company, p. 825 (1985).

67. Upthegrove, G., and Burghoff, H. L., <u>Elevated-Temperature Properties of Copper and Copper-Base Alloys</u>, ASTM Special Technical Publication, No. 181, p. 123 (1956)

68 Wilkins, R. A., Bunn, E. S., <u>Copper and Copper Base Alloys- The Physical and Mechanical Properties of Copper and its Commercial Alloys in Wrought Form</u>, McGraw-Hill Book Company, Inc., New York and London, p. 27 (1943).

69. Hultgren, H., and Desai, P. D. <u>Selected Thermodynamic Values and Phase Diagrams for Copper and Some of its Binary Alloys</u>, NSRDS, p. 193 (1971).

Table III. Tensile strength of different alloys on HTTM and 410.31 model MTS.

Alloy	Tensile Strength on HTTM (ksi)	Tensile Strength on MTS (ksi)
C46400	63	64
	64	
7075-T651	86	83
	86	
	87	
6061-T651	48	45
	47	
AZ31B	41	38

VITA

NARESH VENKATA LAKSHMI ADURTY

Candidate for the Degree of

Master of Science

Thesis: EMBRITTLEMENT OF C46400 BRASS BY LIQUID MERCURY

Major Field: Mechanical Engineering

Biographical:

Personal Data: Born in Jamshedpur, India, On January 9, 1970, the son of Kameshwar Rao and Nageshwari Adurty.

Education: Graduate from Kendriya Vidyalaya, Secunderabad, India, 1985; received Bachelor of Engineering Degree in Mechanical Engineering from Kakatiya University, Warangal, India, in July 1991; completed requirements for Master of Science at Oklahoma State University in May 1994.

Experience: Employed by Oklahoma State University, Department of Mechanical and Aerospace Engineering as a Teaching Assistant from August 1992 to May 1993.

Professional Memberships: American Society of Mechanical Engineers, Society of Manufacturing Engineers.